Fine structure of neutral and charged excitons in self-assembled In(Ga)As/(Al)GaAs quantum dots

M. Bayer,* G. Ortner, O. Stern, A. Kuther, A. A. Gorbunov,† and A. Forchel
Technische Physik, Universität Würzburg, Am Hubland, D-97074 Würzburg, Germany

P. Hawrylak, S. Fafard, and K. Hinzer
Institute for Microstructural Sciences, National Research Council, Ottawa O1A R6, Canada

T. L. Reinecke and S. N. Walck‡
Naval Research Laboratory, Washington, DC 20375

J. P. Reithmaier, F. Klopf, and F. Schäfer
Technische Physik, Universität Würzburg, Am Hubland, D-97074 Würzburg, Germany
(Received 4 July 2001; published 7 May 2002)

The fine structure of excitons is studied by magnetophotoluminescence spectroscopy of single self-assembled In(Ga)As/(Al)GaAs quantum dots. Both strength and orientation of the magnetic field are varied. In a combination with a detailed theoretical analysis, these studies allow us to develop a comprehensive picture of the exciton fine structure. Symmetry of the dot structures as well as its breaking cause characteristic features in the optical spectra, which are determined by the electron-hole exchange and the Zeeman interaction of the carriers. The symmetry breaking is either inherent to the dot due to geometry asymmetries, or it can be obtained by applying a magnetic field with an orientation different from the dot symmetry axis. From data on spin splitting and on polarization of the emission we can identify neutral as well as charged exciton complexes. For dots with weakly broken symmetry, the angular momentum of the neutral exciton is no longer a good quantum number and the exchange interaction lifts degeneracies within the fine-structure manifold. The symmetry can be restored by a magnetic field due to the comparatively strong Zeeman interactions of electron and hole. For dots with a strongly broken symmetry, bright and dark excitons undergo a strong hybridization, as evidenced by pronounced anticrossings when states within the manifold are brought into resonance. The fine structure can no longer be described within the frame developed for structures of higher dimensionality. In particular, the hybridization cannot be broken magnetically. For charged excitons, the exchange interaction vanishes, demonstrating that the exchange splitting of a neutral exciton can be switched off by injecting an additional carrier.

DOI: 10.1103/PhysRevB.65.195315 PACS number(s): 71.35.Ji, 71.70.Ej, 71.70.Gm

I. INTRODUCTION

Optical excitation of a semiconductor lifts an electron across the band gap and leaves a hole in the valence band. Electron and hole bind to form an exciton through their mutual Coulomb interaction. Each of the excitonic levels consists of a multiplet of states corresponding to different spin configurations of the carriers. The multiplet exhibits a fine-structure splitting that is caused by two contributions: the exchange interaction, which couples the spins of electron and hole, and their Zeeman interaction with an (external or internal) magnetic field. The multiplet splitting is largely determined by the symmetry of the structures, which can result in characteristic degeneracies among the exciton states. Despite the interest in this, the resolution of the fine structure has only been partly possible in spectroscopic experiments because of the magnitude of the energies involved, which typically are considerably smaller than the inhomogeneous broadening, particularly in bulk and quantum wells. Spectroscopy of single quantum dots[1–50] opens up possibilities for a more detailed study because of the suppression of inhomogeneities. In addition, its resolution is further facilitated because the exchange interaction energies are drastically enhanced by quantum confinement.

Quantum dots[51] can be fabricated by several techniques, among which self-assembled growth[52] has been shown to be particularly promising because of the high optical quality of the resulting dot structures. For these, the study of single self-assembled dots is complicated by the rather high dot densities, which result in mean dot separations of the order of tens to hundreds of nanometers. Therefore, techniques are required which provide the corresponding spatial resolution. During recent years great progress has been made in the development of experimental tools which allow such studies. Among them are sophisticated spectroscopic techniques such as confocal microscopy, by which single structures can be addressed for samples with rather low dot densities. Another technique is near-field scanning microscopy, which provides a spatial resolution clearly below the wavelength of light, so that high-density samples also can be investigated.

Single-dot spectroscopy can also be obtained by a further technological processing of as-grown quantum dot samples. For example, the dots could be covered by a mask containing small apertures through which the optical excitation as well as the collection of the signal is done. Another possibility is offered by a lateral patterning of the dot structures. In this way small mesa structures can be fabricated which contain only a single quantum dot or a few quantum dots, and which then can be addressed by conventional far-field spectroscopy.

These techniques have been used to obtain insight into a

variety of problems such as the coupling of excitons to phonons or the binding energies of excitonic complexes.[51] Steps toward a complete understanding of the exciton fine structure have also been taken: In studies of single quantum dots formed at GaAs/$Al_xGa_{1-x}As$ interfaces, a splitting of the ground and excited exciton states was reported, which arises from the long-range electron-hole exchange interaction.[6] The understanding of the relation between the fine structure and the dot symmetry was extended by recent investigations of self-assembled In(Ga)As/GaAs,[19] CdSe/ZnSe,[20,22] InP/Ga_yInP_{1-y},[21] and CdTe/$Cd_zMg_{1-z}Te$[28] quantum dots. It has been shown that a reduction of the quantum dot symmetry lifts degeneracies among the exciton states, and also influences the polarization of their emission.

Exciton spin splittings in magnetic field have been studied for several types of quantum dots.[7,11,15,16,22] It was found that the underlying *g* factors differ strongly from those in bulk or quantum wells. However, up to now no complete understanding of *g* factors has been reported, to our knowledge.[53] The potential of single-dot spectroscopy was particularly evidenced by experiments in which a subtle effect such as the interaction of the exciton spin with the spins of the lattice nuclei was investigated.[7] This interaction causes a shift of the exciton energy (the Overhauser shift), corresponding to an effective internal magnetic field which can be as large as ~ 2 T.

Single-dot spectroscopy also permitted the study of complexes formed from a larger number of electrons and holes: Biexcitonic contributions to the optical spectrum could be identified for various types of quantum dots, e.g., in high excitation photoluminescence[1,13–15,20,23,28,29] and in two-photon-absorption.[1] It was demonstrated that the fine structure of the biexciton emission is identical to that of the exciton because the biexciton is a spin-singlet state and exhibits neither exchange nor Zeeman interaction splitting.[15,20,28] Therefore, in the optical spectra any fine structure of the emission is fully determined by the fine structure of the exciton in the final state of the electron-hole recombination.

Here we have performed magnetophotoluminescence spectroscopy on different types of self-assembled In(Ga)As/(Al)GaAs single quantum dots. From these studies we obtain detailed insights into the exchange and Zeeman interactions of the carriers forming excitons and exciton complexes. In particular, we will demonstrate for charge neutral excitons that both short- and long-ranged parts of the exchange interaction are required to describe the experimental observations. One main effect of the short-ranged part is a splitting of the exciton multiplett into bright and dark subspaces (independent of the dot symmetry), while the long-ranged part results in a splitting of the bright excitons in asymmetric dots besides contributing to the bright-dark splitting. Generally it is believed that the short-range interaction is not important for asymmetry splittings, which has been confirmed for structures of higher dimensionality. By observing a considerable splitting of the dark excitons, we will demonstrate that this description is too simplified for quantum dots. For charged excitons, we will show that the exchange energies vanish due to the interaction of an electron (a hole) with a spin-singlet state formed by two holes (two electrons). This means that the exchange interaction which couples the spins of an electron and a hole in a neutral exciton can be switched off in strongly confined quantum dots by adding an additional carrier.

The main goal of this paper is less the quantitative determination of the fine-structure parameters such as exchange energies or *g* factors (which vary with the studied quantum dot type, and which yet cannot be easily related to quantum dot properties such as size and shape due to the lack of corresponding knowledge for self-assembled dots), rather than the development of different scenarios for the exciton fine-structure patterns and their relation to the dot symmetry. We note that all the quantum dots from the different studied samples could be categorized according to these scenarios. The outline of the paper is the following: In Sec. II an analysis of the fine structure will be given for quantum dots of different symmetries. A description of the studied samples as well as the experimental technique is given in Sec. III. In Sec. IV we will then present the spectroscopic data for the various quantum dot structures and compare them with the theoretical expectations.

II. ANALYSIS OF THE FINE STRUCTURE

A. Neutral excitons

The exciton fine structure[54–70] at zero magnetic field arises from the exchange interaction, which couples the spins of the electron and hole. In its general form the exchange energy is proportional to the integral

$$E_{exchange} \propto \int\int d^3r_1 d^3r_2 \Psi_X^*(\mathbf{r}_e=\mathbf{r}_1,\mathbf{r}_h=\mathbf{r}_2) \times \frac{1}{|\mathbf{r}_1-\mathbf{r}_2|} \Psi_X(\mathbf{r}_e=\mathbf{r}_2,\mathbf{r}_h=\mathbf{r}_1),$$

where Ψ_X is the exciton wave function and $\mathbf{r}_{e,h}$ are the electron and hole coordinates. When calculating the exchange, for technical reasons the integral is divided in two parts, for which there are two possibilities: First it can be divided in real space into short- and long-ranged parts. The short-ranged part is given by the probability of finding an electron and a hole in the same Wigner-Seitz unit cell, and conversely the long-ranged part is the contribution when they are in different cells. Second, the integral can also be divided in *k* space, which gives analytical and nonanalytical parts. These two formal separations are closely related to one another, although they are not fully identical.

In magnetic field *B* the fine structure is extended by the Zeeman interaction of the electron and hole spins with *B*.[63,64,55] We note that in general the interaction of the carrier spins with the spins of the lattice nuclei also needs to be included in the discussion. This results in the well-known Overhauser shift of the exciton energy.[7] For its observation, the optically generated excitons have to be spin polarized to align the spins of the lattice nuclei. This may be obtained by a resonant optical excitation of the quantum dots using cir-

cularly polarized light. In the experiments described below, however, nonresonant excitation with linearly polarized light was used. Consequently the time-averaged spin polarization is zero and the lattice is depolarized. Therefore, this part of the fine structure interaction is neglected here.

In the following we will first analyze the short-ranged part, for which we will use the method of invariants reported by van Kasteren *et al.* for quantum-well structures having a given symmetry.[63] The quantum dots studied in the present work are to a good approximation lens shaped, with a height-to-width ratio of $\sim 1:3$; therefore, that analysis should be applicable to the dot case as well. It can also be used for describing the interaction of the carrier spins with an external magnetic field. In it, for coupling carrier spins and for coupling spins to B the most general multiplicative forms of the angular momentum operators of the electron and hole are chosen so that they are invariant under the transformations of the symmetry group describing the system. The long-ranged exchange interaction can be easily included in the discussion because it ''exhibits the same spin structure,'' that is, its contributions can simply be added to the terms of the short-ranged interaction.

Dot structures exhibiting different symmetries will be considered: In addition to dots of high symmetry belonging to the D_{2d} group, dots with lower symmetry will also be studied. These structures could belong to the $C_{2,v}$ or C_2 groups, or could even show no symmetry at all. D_{2d} is the symmetry of dots with an in-plane rotational invariance. Their symmetry could be broken down to $C_{2,v}$ or C_2 by an uniaxial deformation, e.g., by strain, so that the dot shape becomes ellipsoidal. In the case of further deformation, the dot structures would lose all symmetry.

1. Zero magnetic field

a. Short-range exchange interaction. First the discussion will concentrate on quantum dots exhibiting specific symmetries. The general form of the spin Hamiltonian for the electron-hole exchange interaction of an exciton formed by a hole with spin J_h and by an electron with spin S_e is given by[63,64,55]

$$\mathcal{H}_{exchange} = -\sum_{i=x,y,z} (a_i J_{h,i} S_{e,i} + b_i J_{h,i}^3 S_{e,i}). \qquad (1)$$

For the following analysis the z direction is chosen to point along the heterostructure growth direction. Due to the strain in self-assembled quantum dots, the heavy- and light-hole states are split in energy by at least several tens of meV. This splitting is considerably larger than the fine-structure interaction energies, and the light-hole states can safely be neglected. The single-particle basis from which the excitons are constructed therefore consists of a heavy hole with $J_h = 3/2$, $J_{h,z} = \pm 3/2$ and an electron $S_e = 1/2, S_{e,z} = \pm 1/2$.[71]

From these states four excitons are formed, which are degenerate when the spin Hamiltonian [Eq. (1)] is neglected. These states are characterized by their angular momentum projections $M = S_{e,z} + J_{h,z}$. States with $|M| = 2$ cannot couple to the light field, and are therefore optically inactive (dark excitons), while states with $|M| = 1$ are optically active (bright excitons). With these angular-momentum eigenstates the matrix representation of $\mathcal{H}_{exchange}$ can be constructed. Due to the neglect of heavy-hole–light-hole mixing, the x and y components that are linear in J_h are omitted.

Using the exciton states $(|+1\rangle, |-1\rangle, |+2\rangle, |-2\rangle)$ as basis, the following matrix representation is obtained:

$$\mathcal{H}_{exchange} = \frac{1}{2}\begin{pmatrix} +\delta_0 & +\delta_1 & 0 & 0 \\ +\delta_1 & +\delta_0 & 0 & 0 \\ 0 & 0 & -\delta_0 & +\delta_2 \\ 0 & 0 & +\delta_2 & -\delta_0 \end{pmatrix}. \qquad (2)$$

Here the following abbreviations have been introduced: $\delta_0 = 1.5(a_z + 2.25 b_z)$, $\delta_1 = 0.75(b_x - b_y)$, and $\delta_2 = 0.75(b_x + b_y)$. The first term of the Hamiltonian $\mathcal{H}_{exchange}$ in Eq. (1) gives the diagonal matrix elements, while the second term gives the off-diagonal elements. The matrix in Eq. (2) has a

TABLE I. Exciton eigenstates in structures of D_{2d} and of lower symmetry. When the long-range interaction is included in the discussion, δ_0 has to be replaced by $\Delta_0 = \delta_0 + \gamma_0$ as well as δ_1 by $\Delta_1 = \delta_1 + \gamma_1$.

D_{2d} $b_x = b_y$		$< D_{2d}$ $b_x \neq b_y$	
Energy	Eigenstate	Energy	Eigenstate
$+\frac{1}{2}\delta_0$	$\|-1\rangle$	$+\frac{1}{2}\delta_0 + \frac{1}{2}\delta_1$	$\frac{1}{\sqrt{2}}(\|+1\rangle + \|-1\rangle)$
$+\frac{1}{2}\delta_0$	$\|+1\rangle$	$+\frac{1}{2}\delta_0 - \frac{1}{2}\delta_1$	$\frac{1}{\sqrt{2}}(\|+1\rangle - \|-1\rangle)$
$-\frac{1}{2}\delta_0 + \frac{1}{2}\delta_2$	$\frac{1}{\sqrt{2}}(\|+2\rangle + \|-2\rangle)$	$-\frac{1}{2}\delta_0 + \frac{1}{2}\delta_2$	$\frac{1}{\sqrt{2}}(\|+2\rangle + \|-2\rangle)$
$-\frac{1}{2}\delta_0 - \frac{1}{2}\delta_2$	$\frac{1}{\sqrt{2}}(\|+2\rangle - \|-2\rangle)$	$-\frac{1}{2}\delta_0 - \frac{1}{2}\delta_2$	$\frac{1}{\sqrt{2}}(\|+2\rangle - \|-2\rangle)$

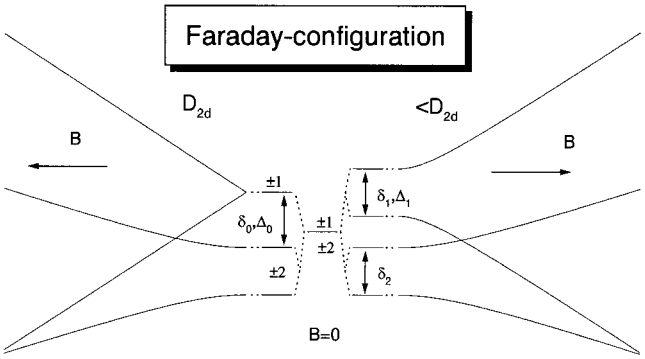

FIG. 1. Scheme of the exciton fine structure at zero magnetic field and in magnetic field. The magnetic field is aligned in the Faraday configuration. The central part of the figure shows the situation at $B=0$ neglecting the spin Hamiltonian [Eq. (1)] (for which the excitons with $M=\pm1$ and ±2 are degenerate) and including it. The left-hand side shows the evolution of the fine structure in the magnetic field for quantum dots with D_{2d} symmetry, while the right-hand side shows the evolution for dots with a symmetry $<D_{2d}$.

block diagonal form. Therefore, dark and bright excitons do not mix with each other, and their energies differ by the electron-hole exchange energy δ_0. Due to the off-diagonal matrix elements in the corresponding subblocks, in general the excitons with each $|M|=1$ and $|M|=2$ are hybridized: Rotational symmetry of the structures studied implies $b_x=b_y$, resulting in $\delta_1=0$. In this case the states $|+1\rangle$ and $|-1\rangle$ are eigenstates of $\mathcal{H}_{exchange}$. If, however, the rotational symmetry is broken ($b_x\neq b_y$), the angular momentum is no longer a good quantum number, and the $M=\pm1$ excitons are mixed with one another. In contrast, the excitons with $|M|=2$ always hybridize, independent of the dot symmetry.

Table I shows the eigenstates and their energies obtained from diagonalizing the exchange Hamiltonian [Eq. (1)]. For structures with D_{2d} symmetry the $|+1\rangle$ and $|-1\rangle$ states are degenerate. On the other hand, for broken symmetry the eigenstates of $\mathcal{H}_{exchange}$ are symmetric and antisymmetric linear combinations of the angular momentum states, and are split from one another by δ_1. The energy splitting between the two hybridized states of $|+2\rangle$ and $|-2\rangle$ is equal to δ_2. The splitting patterns are shown schematically in the central part of Fig. 1 for quantum dots with D_{2d} and with lower symmetry. For the splittings between the exciton doublets, $\delta_2>\delta_1$ holds exactly. In general, both splittings should be rather small compared to δ_0, because they are given by the coupling matrix elements that are proportional to J_h^3.

a. Long-range exchange interaction. The main effect of the short-ranged exchange interaction (independent of the symmetry of the structures) is a splitting of the exciton multiplet into bright and dark pairs of states. The effect of the long-ranged part, on the other hand, is twofold: First, it contributes to the splitting of the bright and dark excitons. Second, it causes a splitting of the bright excitons in structures with symmetry $<D_{2d}$ in transverse and longitudinal components, while it does not influence the dark states. In the zero-field Hamiltonian $\mathcal{H}_{exchange}$ of Eq. (2) it can be included

TABLE II. Exciton eigenstates in the magnetic field (Faraday configuration) in structures of D_{2d} symmetry. $\beta_1=\mu_B(g_{e,z}+g_{h,z})B_z$ and $-\beta_2=\mu_B(g_{e,z}-g_{h,z})B_z$. The normalization constants N_3 and N_4 depend on the magnetic field.

D_{2d}	
Energy	Eigenstate
$+\frac{1}{2}\delta_0+\frac{1}{2}\beta_1$	$\|-1\rangle$
$+\frac{1}{2}\delta_0-\frac{1}{2}\beta_1$	$\|+1\rangle$
$-\frac{1}{2}\delta_0+\frac{1}{2}\sqrt{\delta_2^2+\beta_2^2}$	$N_3[\|+2\rangle+\left(\frac{\beta_2}{\delta_2}+\sqrt{1+\frac{\beta_2^2}{\delta_2^2}}\right)\|-2\rangle]$
$-\frac{1}{2}\delta_0-\frac{1}{2}\sqrt{\delta_2^2+\beta_2^2}$	$N_4[\|+2\rangle+\left(\frac{\beta_2}{\delta_2}-\sqrt{1+\frac{\beta_2^2}{\delta_2^2}}\right)\|-2\rangle]$

easily by adding the corresponding energies to the off-diagonal matrix elements in the subblock of the $|M|=1$ excitons. This subblock then is given by[63,64,55]

$$\begin{pmatrix} +\Delta_0 & +\Delta_1 \\ +\Delta_1 & +\Delta_0 \end{pmatrix}, \tag{3}$$

with $\Delta_0=\delta_0+\gamma_0$, where γ_0 is the contribution of the long-range exchange to the splitting between dark and bright excitons. Further, $\Delta_1=\delta_1+\gamma_1$, $\gamma_1=(\gamma_x-\gamma_y)$, where the γ_i, $i=x,y$ are the coupling constants of the long-range interaction. Thus, for it to become important, a dot asymmetry is required. For dot structures that exhibit rotational symmetry ($\gamma_x=\gamma_y$) it vanishes, as does the short-ranged part δ_1. The principal scheme of the fine-structure splitting given in Fig. 1 remains unchanged by the inclusion of the long-range interaction, except for an enhancement of the splitting of the bright exciton doublet. From this splitting the relative importance of the two contributions to the exchange interaction cannot be traced. In general it is assumed that $\gamma_1\gg\delta_1$. The influence of the cubic terms in the short-range interaction could, however, be determined from a splitting of the dark exciton doublet.

2. Nonzero magnetic field

The general form of the interaction of the electron and hole spins with an external magnetic field $\mathbf{B}=(B_x,B_y,B_z)$ of arbitrary strength and orientation is given by[63,64,55]

$$\mathcal{H}_{zeeman}(B)=-\mu_B\sum_i\,(+g_{e,i}S_{e,i}-2\kappa_iJ_{h,i}-2q_iJ_{h,i}^3)B_i\,.$$

μ_B is the Bohr magneton. q_i and κ_i are the valence-band parameters in the Luttinger-Kohn Hamiltonian ($\kappa_i\gg q_i$).

a. Faraday configuration. First the Faraday configuration will be considered, in which the magnetic field is oriented along the heterostructure growth direction ($B\|z$). Due to the restriction to heavy-hole excitons, the Hamitonian can be simplified by making use of $J_{h,z}^2=9/4$:

$$\mathcal{H}_{zeeman}^F(B)=-\mu_B\left(g_{e,z}S_{e,z}-\frac{g_{h,z}}{3}J_{h,z}\right)B_z\,. \tag{4}$$

The effective hole g factor $g_{h,z}$ is related to the Luttinger-Kohn parameters by $g_{h,z}=6\kappa_z+13.5q_z$.[72] Again using the basis of exciton states from Sec. II A 1, the matrix describing the Zeeman interaction is given by

$$\mathcal{H}^F_{zeeman}(B)=\frac{\mu_B B_z}{2}\begin{pmatrix} +(g_{e,z}+g_{h,z}) & 0 & 0 & 0 \\ 0 & -(g_{e,z}+g_{h,z}) & 0 & 0 \\ 0 & 0 & -(g_{e,z}-g_{h,z}) & 0 \\ 0 & 0 & 0 & +(g_{e,z}-g_{h,z}) \end{pmatrix}.$$

The matrix has a diagonal form because of the rotational symmetry of the Hamiltonian around the z axis. The total Hamiltonian of the system is obtained by adding $\mathcal{H}^F_{zeeman}(B)$ to $\mathcal{H}_{exchange}$. Here the strength of the diagonal matrix elements can be tuned relative to the strength of the off-diagonal ones through the magnetic-field dependence of the Zeeman interaction.

Tables II (for D_{2d} symmetry) and III (for broken D_{2d} symmetry) show the exciton energies and eigenstates in a magnetic field. Here the definitions $\beta_1=\mu_B(g_{e,z}+g_{h,z})B_z$ and $-\beta_2=\mu_B(g_{e,z}-g_{h,z})B_z$ have been used. For a quantum dot with D_{2d} symmetry the spin splitting of the ± 1 states increases linearly with increasing magnetic field. For the dark excitons, the spin splitting shows a nonlinear dependence on B because of the hybridization of the $|M|=2$ excitons at zero field. For an asymmetric quantum dot of lower symmetry the $|M|=1$ exciton states are linear combinations of the angular-momentum eigenstates, where the coefficients depend on the magnetic field. Their energy splitting deviates from a linear dependence: For low fields it varies quadratically with B. Only for high fields, for which the Zeeman interaction energies are considerably larger than the exchange energies $\delta_1(\Delta_1)$, is a linear field dependence found for the spin splitting. The left and right parts of Fig. 1 show the evolution of the exciton fine structure splitting in a magnetic field (the Faraday configuration). We note that due to their different symmetries the lower-energy level of the bright excitons and the upper level of the dark excitons cross each other with increasing field.

b. Voigt configuration. An orientation of the magnetic field perpendicular to the heterostructure growth direction, i.e., in the x-y plane, changes the matrix representation of the Zeeman interaction significantly. For the analysis we will neglect terms which are cubic in the hole momentum. Their coefficients q_i are small as compared to κ_i for quantum dots of high symmetry, which are of interest in the corresponding experiments described below. For simplicity we consider only the case of a magnetic field aligned either along the x or y direction. The matrix representations of the corresponding Hamiltonians are written as

$$\mathcal{H}^V_{zeeman,x}=\frac{\mu_B B_x}{2}\begin{pmatrix} 0 & 0 & g_{e,x} & g_{h_2,x} \\ 0 & 0 & g_{h_2,x} & g_{e,x} \\ g_{e,x} & g_{h_2,x} & 0 & 0 \\ g_{h_2,x} & g_{e,x} & 0 & 0 \end{pmatrix},$$

TABLE III. Excitonic states in the magnetic field in structures with symmetry lower than D_{2d} (Faraday configuration). $\beta_1=\mu_B(g_{e,z}+g_{h,z})B_z$ and $-\beta_2=\mu_B(g_{e,z}-g_{h,z})B_z$. The normalization constants N_i, $i=1,\ldots,4$ depend on the magnetic field.

$<D_{2d}$	
Energy	Eigenstate
$+\frac{1}{2}\delta_0+\frac{1}{2}\sqrt{\delta_1^2+\beta_1^2}$	$\lvert L_1\rangle=N_1[\lvert+1\rangle+\left(\frac{\beta_1}{\delta_1}+\sqrt{1+\frac{\beta_1^2}{\delta_1^2}}\right)\lvert-1\rangle]$
$+\frac{1}{2}\delta_0-\frac{1}{2}\sqrt{\delta_1^2+\beta_1^2}$	$\lvert L_2\rangle=N_2[\lvert+1\rangle+\left(\frac{\beta_1}{\delta_1}-\sqrt{1+\frac{\beta_1^2}{\delta_1^2}}\right)\lvert-1\rangle]$
$-\frac{1}{2}\delta_0+\frac{1}{2}\sqrt{\delta_2^2+\beta_2^2}$	$N_3[\lvert+2\rangle+\left(\frac{\beta_2}{\delta_2}+\sqrt{1+\frac{\beta_2^2}{\delta_2^2}}\right)\lvert-2\rangle]$
$-\frac{1}{2}\delta_0-\frac{1}{2}\sqrt{\delta_2^2+\beta_2^2}$	$N_4[\lvert+2\rangle+\left(\frac{\beta_2}{\delta_2}-\sqrt{1+\frac{\beta_2^2}{\delta_2^2}}\right)\lvert-2\rangle]$

TABLE IV. Excitonic states in the magnetic field in structures of symmetry lower than D_{2d} (Voigt configuration $\vec{B}\|\vec{e}_x$). The coefficients α_i and the normalization constants N_i are functions of the magnetic field. The α_i, $i=1,\ldots,4$ vanish in the limit of zero magnetic field, because the state mixing is caused by the magnetic field.

$<D_{2d}$	
Energy	Eigenstate
$+\frac{1}{4}[+(\delta_1+\delta_2)+\sqrt{(2\delta_0+\delta_1-\delta_2)^2+4(g_{e,x}-g_{h,x})^2\mu_B^2B^2}]$	$N_1[(\lvert+1\rangle-\lvert-1\rangle)+\alpha_1(\lvert+2\rangle-\lvert-2\rangle)]$
$+\frac{1}{4}[-(\delta_1+\delta_2)+\sqrt{(2\delta_0-\delta_1+\delta_2)^2+4(g_{e,x}+g_{h,x})^2\mu_B^2B^2}]$	$N_2[(\lvert+1\rangle+\lvert-1\rangle)+\alpha_2(\lvert+2\rangle+\lvert-2\rangle)]$
$-\frac{1}{4}[-(\delta_1+\delta_2)+\sqrt{(2\delta_0+\delta_1-\delta_2)^2+4(g_{e,x}-g_{h,x})^2\mu_B^2B^2}]$	$N_3[(\lvert+2\rangle-\lvert-2\rangle)+\alpha_3(\lvert+1\rangle-\lvert-1\rangle)]$
$-\frac{1}{4}[+(\delta_1+\delta_2)+\sqrt{(2\delta_0-\delta_1+\delta_2)^2+4(g_{e,x}+g_{h,x})^2\mu_B^2B^2}]$	$N_4[(\lvert+2\rangle+\lvert-2\rangle)+\alpha_4(\lvert+1\rangle+\lvert-1\rangle)]$

$$\mathcal{H}^V_{zeeman,y}=i\frac{\mu_B B_y}{2}\begin{pmatrix}0 & 0 & g_{e,y} & -g_{h_2,y}\\ 0 & 0 & g_{h_2,y} & -g_{e,y}\\ -g_{e,y} & g_{h_2,y} & 0 & 0\\ -g_{h_2,y} & g_{e,y} & 0 & 0\end{pmatrix}.$$

Due to the pseudovector character of the magnetic field, the following relations hold for the in-plane electron and hole g factors in symmetric quantum dots: $g_{e,x}=-g_{e,y}$ and $g_{h,x}=-g_{h,y}$. Only under these conditions is the Hamiltonian invariant with respect to in-plane rotations of 90°. In contrast to the Faraday configuration, the matrix now has off-diagonal elements. The in-plane magnetic field destroys the rotational symmetry, and causes a mixing of bright and dark excitons, resulting in the observability of the ''dark'' states in the spectra. In a classical picture the carriers react to B_x, or respectively to B_y, by a precession of the carrier spins around the field. Due to the precession of the electron spin the $+1$ (-1) exciton couples to the $+2$ (-2) exciton, while the precession of the hole couples the $+1$ and the -2 excitons as well as the -1 and the $+2$ excitons. Eigenstates and energies for the Voigt configuration are given in Tables IV ($B\|x$) and V ($B\|y$). Figure 2 shows a sketch of the exciton fine structure in the Voigt configuration. For simplicity we have assumed that the exchange energy splittings δ_1 (Δ_1) and δ_2 are negligibly small (which is in good approximation valid for D_{2d} symmetry). In contrast to the crossing behavior observed for the Faraday configuration, the spin splitting now shows a kind of anticrossing behavior. The excitons which are bright at $B=0$ both shift to higher energies with increasing magnetic field, while the energies of the $|M|=2$ excitons are lowered by B. Consequently, the energy splittings between the exciton states increase.

3. Complete symmetry breaking

Finally let us discuss the case of a fully broken symmetry of the quantum dots. Such a symmetry breaking could be obtained, for example, by a very inhomogeneous strain distribution. In this case the method of invariants is no longer appropriate to analyze the exciton fine structure. Here we intend to give only a qualitative analysis of this situation. The classification of the exciton states as dark and bright ones becomes impossible, the complete breaking of the rotational symmetry causes a mixing of the four band-edge exciton states, due to which all become observable in the optical spectra. Because of this mixing, in the Faraday configuration one no longer expects a crossing of the states corresponding to the $M=-1$ and the $+2$ excitons when they approach each other with increasing magnetic field. Instead, an anticrossing of these states should be observed. To restore the rotational symmetry, high-magnetic-field strengths are required, resulting in a interaction of the carrier spins with B so strong that the spins are effectively decoupled and exchange can be neglected.

B. Charged excitons

As an example of a trion complex,[73,74] here we consider the negatively charged trion X^-. The arguments for this can be easily transferred to the positively charged exciton X^+. In its lowest-energy state, X^- consists of two electrons of op-

TABLE V. Excitonic states in the magnetic field in structures of symmetry lower than D_{2d} (Voigt configuration $\vec{B}\|\vec{e}_y$). The coefficients β_i and the normalization constants N_i are complicated functions of the magnetic field.

$<D_{2d}$	
Energy	Eigenstate
$+\frac{1}{4}[+(\delta_1-\delta_2)+\sqrt{(2\delta_0+\delta_1+\delta_2)^2+4(g_{e,y}-g_{h,y})^2\mu_B^2B^2}]$	$N_1[(\lvert+1\rangle-\lvert-1\rangle)+i\beta_1(\lvert+2\rangle+\lvert-2\rangle)]$
$+\frac{1}{4}[-(\delta_1-\delta_2)+\sqrt{(2\delta_0-\delta_1-\delta_2)^2+4(g_{e,y}+g_{h,y})^2\mu_B^2B^2}]$	$N_2[(\lvert+1\rangle+\lvert-1\rangle)+i\beta_2(\lvert+2\rangle-\lvert-2\rangle)]$
$-\frac{1}{4}[+(\delta_1-\delta_2)+\sqrt{(2\delta_0-\delta_1-\delta_2)^2+4(g_{e,y}+g_{h,y})^2\mu_B^2B^2}]$	$N_3[(\lvert+2\rangle-\lvert-2\rangle)+i\beta_3(\lvert+1\rangle+\lvert-1\rangle)]$
$-\frac{1}{4}[-(\delta_1-\delta_2)+\sqrt{(2\delta_0+\delta_1+\delta_2)^2+4(g_{e,y}-g_{h,y})^2\mu_B^2B^2}]$	$N_4[(\lvert+2\rangle+\lvert-2\rangle)+i\beta_4(\lvert+1\rangle+\lvert-1\rangle)]$

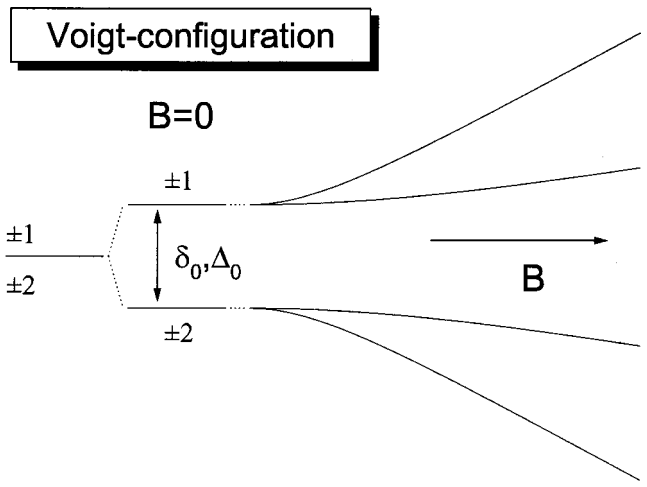

FIG. 2. Scheme of the exciton fine structure in a magnetic field aligned in the Voigt configuration. Here only the case of quantum dots of high symmetry D_{2d} is shown, for which the dot-asymmetry-induced exchange energy splittings δ_1 and Δ_1 of the bright excitons as well as the hybridization energy δ_2 of the dark excitons vanish.

posite spin and a hole with two possible spin orientations, all carriers being in their ground single-particle states. The complex can be considered as a hole interacting with a spin-singlet electron pair. Therefore, the exchange energy splitting at zero field should vanish (at least for quantum dots in the strong confinement regime, which is the case for the structures studied here). For the emission spectrum, not only the initial state but also the final state after recombination of an electron-hole pair are important, as demonstrated for the emission of the biexciton complex. This final state is given by a single electron. Consequently no exchange energy splitting is observed in the emission of X^-.

We want to point out that we expect this cancellation of the exchange for quantum dots in the strong confinement regime only. Then, in the spin-singlet state, the wave functions of the two electrons in the trion have about the same spatial distributions, leading to a zero local spin density of the electrons. In weakly confined dots as well as in structures of higher dimensionality, on the other hand, the Coulomb interaction might cause a strong mixing of the ground state with higher-lying orbitals and a corresponding redistribution of the carrier wave functions, so that the local spin density might be different from zero.

A magnetic field causes a spin splitting of the X^- exciton state. In the initial state the splitting is given by that of the hole, and in the final state by that of the electron. As a result, the splitting of the emission line is identical to the splitting of a neutral exciton, because it is given by the g factor of the recombining electron hole pair. The g factor of this electron-hole pair is identical to that of an exciton, as long as the electronic band structure is identical to that of an uncharged dot. If the excess carrier originates from an impurity in the dot or close to it, this impurity might lead to a change of the band structure, in particular of the band mixing, and thus to a change of the g factors. Similarly to the case of a neutral exciton, for symmetric quantum dots only the recombination of an electron-hole pair with an angular momentum ± 1 is allowed, if the magnetic field is aligned in the Faraday configuration. If this symmetry is destroyed by confinement potential asymmetries, however, a mixing of angular momentum states may occur activating the ''dark'' part of the charged exciton complex.

TABLE VI. Nominal parameters of the different quantum dot samples studied in the present experiments.

	Dot material	Barrier material
Sample A	$In_{0.60}Ga_{0.40}As$	GaAs
Sample B	InAs	GaAs
Sample C	InAs	$Al_{0.30}Ga_{0.70}As$

Similar to the case of a neutral exciton, such an activation naturally is possible when the field is aligned in the Voigt configuration. Such experiments are a clear criterion of whether an excitonic complex is neutral or charged, independent of the dot symmetry: When the energies of the bright and dark exciton converge for $B \rightarrow 0$, in contrast to the situation sketched in Fig. 2, this can only be explained by emission from trions. Summarizing the considerations, the fine structure of the charged ground-state exciton recombination is obtained from that of an exciton by setting the exchange energy splittings to zero.

Recently there have been reports of a strong suppression of the spin relaxation in quantum dots.[75,76] Thereby the case of a charged exciton becomes more involved, since it might be in an excited state. As an example, here we will discuss a complex consisting of an exciton in the quantum dot ground shell plus an electron in the first excited shell. When the electron in the higher shell has a spin orientation identical to that of the electron in the ground shell, its relaxation is blocked as long as no spin relaxation occurs, and an excited X^- complex is formed. This electron triplet will have Coulomb interactions different from those in the ground state X^-, which is an electron-singlet state. The energy difference between these two complexes will be reflected in the emission spectrum, which arises from the recombination of the electron-hole pair in the ground shell. Again only the configurations with $M = \pm 1$ can be observed in symmetric structures, whereas a symmetry breaking causes the observability of the dark configurations. Analogous to the case of a charge neutral exciton, the dark and bright states are separated by the electron-hole exchange interaction. Further, a quantum dot asymmetry will lead to an exchange splitting of the bright exciton part. Applying a magnetic field, each configuration, the bright one and the dark one, splits into a doublet in the emission spectrum. The spin splitting will be the same as for a neutral exciton because it is given by the *s*-shell recombination.

III. SINGLE-DOT SPECTROSCOPY

In the present work different types of self-assembled In(Ga)As/(Al)GaAs quantum dots have been studied by magnetophotoluminescence spectroscopy. The compositional parameters of the samples are given in Table VI. We emphasize that all the samples are nominally undoped. The first

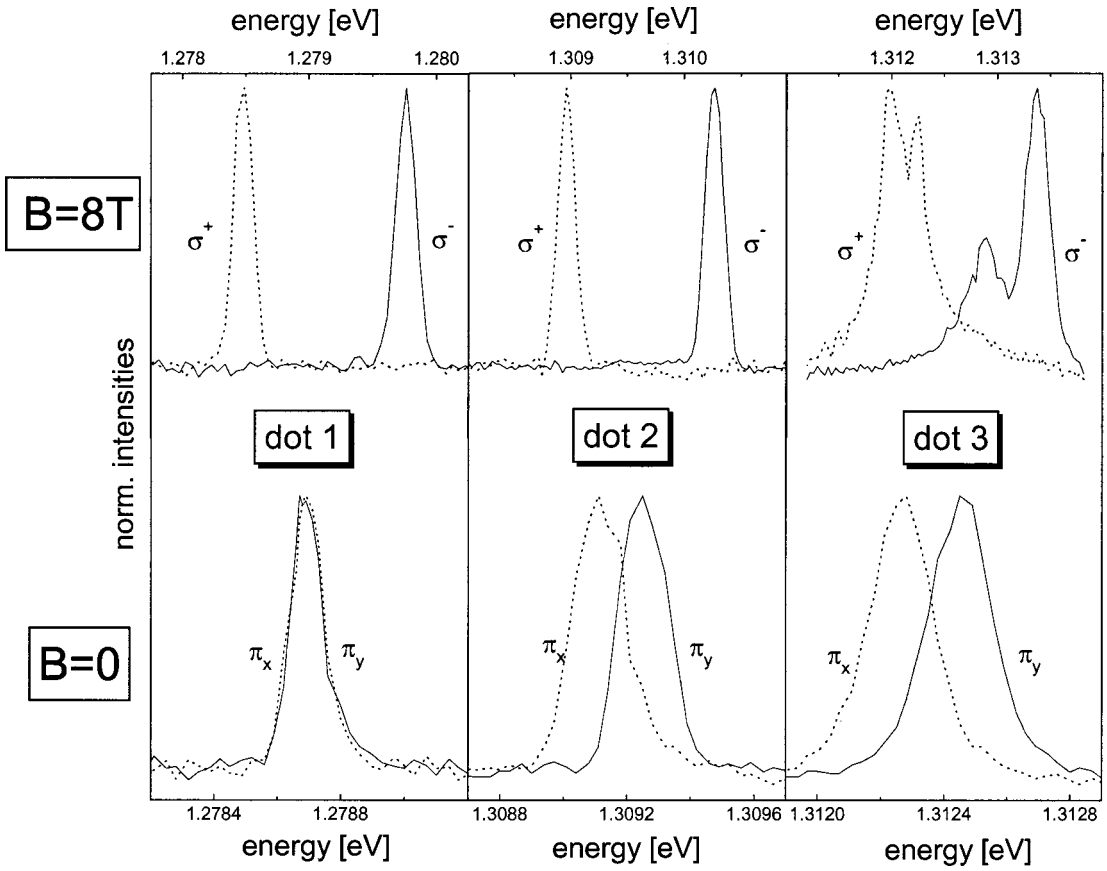

FIG. 3. Polarized photoluminescence spectra of three different $In_{0.60}Ga_{0.40}As/GaAs$ self-assembled single quantum dots (the several panels), each representing a class of dots with a specific fine structure pattern at $B=0$ (lower traces) and at 8 T (upper traces). The zero-field emission has been analyzed with respect to its linear polarization, and for the high-field emission the circular polarization has been detected.

type of structures were $In_{0.60}Ga_{0.40}As$ dots embedded in a GaAs matrix,[77] and the second were InAs dots embedded in GaAs.[78] Finally, we have also studied InAs quantum dots surrounded by an $Al_{0.30}Ga_{0.70}As$ matrix.[79] We want to point out that all these structures are quantum dots in the strong confinement regime, that is, the exciton radius is considerably larger than the dot radius. This results in energy splittings between the confined single-particle shells (that can be estimated from high excitation photoluminescence studies of dot arrays) which are about a factor 2 larger than the exciton binding energy.

Lithography was used to fabricate small mesa structures on the as-grown samples.[15,19] By varying the lateral mesa sizes down to ~ 100 nm, a single quantum dot or very few quantum dots could be isolated and studied by conventional far-field spectroscopy. For these experiments the quantum dots were held in the liquid helium insert ($T=1.5$ K) of an optical split-coil magnetocryostat ($B \leqslant 8$ T). The orientation of the magnetic field could be varied relative to the heterostructure growth direction. For optical excitation a cw Ar^+ laser was used. The illumination power was limited to about 100 μW in order to create only single electron-hole pairs in the dot structures. The emission of the dots was dispersed by a double monochromator with a focal length of 0.6 m, and detected by a liquid-nitrogen-cooled charge-coupled devices camera with a Si chip. The polarization of the emission could be analyzed by a quarter wave retarder and linear polarizers.

Comparing the recorded single-dot spectra we find that the observed spectral half-widths vary from slightly less than 40 to more than 200 μeV. In any case they are clearly larger than the half-widths expected from the radiative lifetimes, which are about 1 ns. Most probably these variations arise from charge fluctuations at the lateral surfaces of the mesa structures: At these surfaces, charges which are created by the laser illumination are trapped, and cause an electric field which results in a Stark shift of the quantum dot energy levels. The surface occupancy with charges varies during recording of the spectrum (typically one minute integration time). Therefore in the spectra an emission band is effectively observed, which is given by the superposition of the several Stark-shifted emission lines (with homogeneously broadened linewidths) corresponding to the different charge distributions. This interpretation is supported by the increase of the half-width when the optical excitation power is increased, which enhances the fluctuations of charge on the surface. This is further supported by the observation of an increase of the half-width with decreasing mesa structure size, leading to an increasing importance of the sidewalls. For a mesa size of about 400 nm we observed the sharpest lines of ~ 35 μeV. In contrast, for the smallest mesa structures with a lateral size of 100 nm, we were unable to observe single-dot emission with a half-width of less than 100 μeV.[80]

IV. DISCUSSION OF THE EXPERIMENTAL DATA

A. Splitting pattern for a neutral exciton

1. Faraday configuration

a. Experimental observations. The three panels of Fig. 3 show polarized photoluminesecence spectra of three different $In_{0.60}Ga_{0.40}As/GaAs$ single quantum dots (sample A) which were recorded at $B=0$ (lower traces) and $B=8$ T (upper traces).[19] The magnetic field was aligned parallel to the heterostructure growth direction. The zero-magnetic-field spectra were analyzed with respect to their linear polarization, while at high fields the circular polarization of the emission was studied. These three quantum dots resemble the three different classes of structures into which all the neutral exciton fine-structure patterns in the $In_{0.60}Ga_{0.40}As/GaAs$ quantum dots can be categorized.[81] The spectra of dots belonging to one class all show the same principal features, although the fine-structure parameters, exchange energies and g factors vary from dot to dot.

The emission from dot 1 (left panel) shows no significant linear polarization at zero magnetic field. In contrast, the emission of the two other quantum dots is split into linearly polarized spectral lines at $B=0$. The splitting between these lines is about 120 μeV for dot 2 (mid panel) and 150 μeV for dot 3 (right panel). In a nonzero magnetic field, the emissions split due to the Zeeman interaction of the exciton spin with B. As a common feature at $B=8$ T, the spectra of all three dots show complete circular polarizations. The low-energy part of the spectrum is σ^+ polarized, and the high-energy one is σ^- polarized. However, the number of spin-split lines varies from dot to dot. For the first two dots a splitting into a doublet is observed, whereas the third dot exhibits a splitting into a quadruplet. Nevertheless, the spin splitting in this case between the two emission features of strong intensity is equal to the spin splittings observed for dots 1 and 2.

b. Discussion. The analysis of the exciton fine structure for quantum dots of different symmetries in Sec. III permits us to understand the features observed for the sample A dots. From the experimental data we find that there are two characteristic quantities from which information about the quantum dot symmetry can be derived: The first quantity is the magnetic-field dependence of the energy splitting between the spectral lines. The second one is the polarization of the emission. Both quantities will be discussed in the following.

The simplest situation is found for dots exhibiting D_{2d} symmetry, for which the exciton angular momentum M is a good quantum number. In this case a single emission line is observed at $B=0$ due to the recombination of the degenerate $M=\pm 1$ excitons, as observed for dot 1. Applying a magnetic field results in a spin splitting. The symbols in Fig. 4 show the observed exciton transition energies as functions of the magnetic field for the three sample A dots of Fig. 3. To facilitate a discussion of the fine-structure effects, we have subtracted the energy of the center of the emission lines for each field strength. This center of emission shifts diamagnetically $\propto B^2$ to higher energies with increasing B. For the $In_{0.60}Ga_{0.40}As/GaAs$ dots the shift is ~ 0.4 meV up to 8 T.

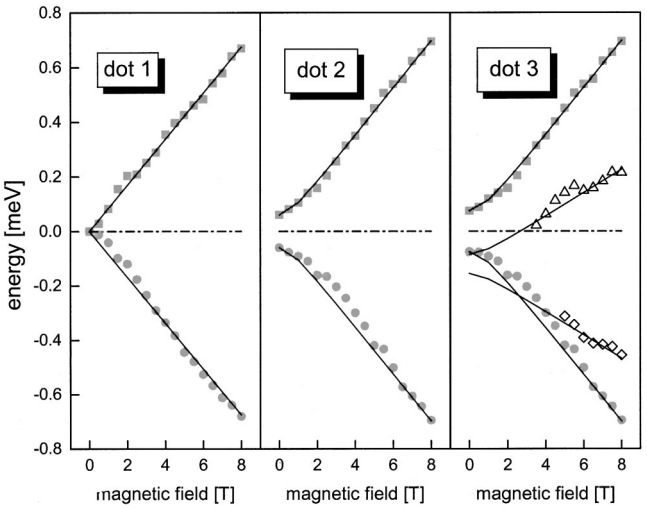

FIG. 4. Exciton transition energies of the three different $In_{0.60}Ga_{0.40}As/GaAs$ self-assembled quantum dots (the several panels) shown in Fig. 3 plotted vs the magnetic field. Symbols give the experimental data, and lines give the results of fits to the data using the forms of the state energies in the exciton fine structure multiplet given in Tables II and III. To focus on the fine-structure effects, the diamagnetic shift of the center of emission has been subtracted in each case.

The symbols in Fig. 5 show the resulting magnetic-field dependencies of the exciton spin splittings $\Delta E=E(\sigma^-)-E(\sigma^+)$. The left panels in Figs. 4 and 5 show the data for dot 1. The dot emission splits linearly into a doublet with increasing B. $\Delta E=+1.4$ meV at 8 T, corresponding to an exciton g factor of -3. The solid lines give the results of fits to the experimental data using the calculated energies in Tables II and III.

The situation becomes more complicated for a dot with a shape deformation for which the rotational symmetry is bro-

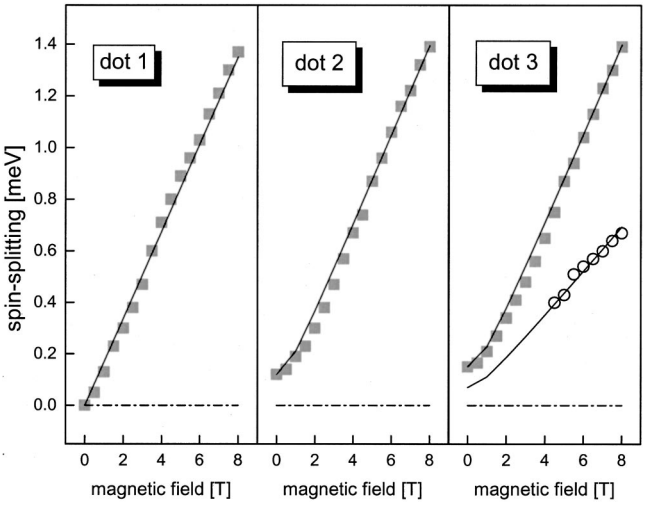

FIG. 5. Magnetic-field dependence of the exciton spin splitting of the three different $In_{0.60}Ga_{0.40}As/GaAs$ single quantum dots shown in Fig. 3 (the several panels). Symbols give the experimental data, and lines the results of fits to the data using the forms obtained from diagonalizing the exciton fine-structure Hamiltonian (Tables II and III).

ken. But still the dot structures shall exhibit symmetries such as $C_{2,v}$ or C_2, so that no mixing of dark and bright excitons occurs. The nonvanishing off-diagonal elements in the subspace of the bright excitons in $\mathcal{H}_{exchange}$ mix the states with $M=+1$ and -1. The new coupled eigenstates repel each other, and the emission from these quantum dots is split by the exchange energy Δ_1, as observed for dot 2 in Fig. 4 (middle panel). From the transition energies we obtain a Δ_1 of about 120 μeV. The magnetic-field dependence of the spin splitting for dot 2 is shown in Fig. 5 (middle panel). In contrast to dot 1, at low B the energy splitting between the exciton transitions increases quadratically with B, and then transforms into a linear dependence. The transition into a linear dependence occurs for about 2 T, because at these field strengths the diagonal Zeeman interaction terms in the Hamiltonian are already considerably larger than the off-diagonal Δ_1. This means that the rotational symmetry is only moderately broken, and it can be easily restored by a magnetic field.

Finally, the behavior of dot 3 with a quadruplet splitting in magnetic field shall be discussed. The observation of four exciton emission lines implies that the dark excitons become visible and that any possible dot symmetry is lifted. This symmetry breaking can have different origins: First, the quantum dot symmetry can be badly broken, so that it exhibits no symmetry at all ($<C_2$). In this case all four band-edge exciton states should already be observable at zero magnetic field. From the spectroscopic data we obtain no clear proof of such a behavior, because at $B=0$ only two emission lines are observed, which are, however, rather broad. In addition, the symmetry breaking could be also magnetic field induced, for which we envisage the following picture: If the dot structure (and therefore its internal [001] crystal axis) is slightly tilted with respect to the heterostructure growth direction, the spectroscopy is effectively no longer performed in Faraday-configuration because there is a field component in the quantum dot plane. This component, which is described by $\mathcal{H}^V_{zeeman,x/y}$, causes a mixing of $|M|=1$ and 2 excitons, making the dark ones visible (see below).

Recent studies revealed that the spin relaxation in quantum dots might be strongly reduced, i.e., the spin relaxation time might become considerably longer than the radiative lifetime of the electron-hole pairs.[75,76] This could result in a significant emission intensity from the predominantly dark excitons (as observed in the experiments for dot 3), although the in-plane field components are rather small, and therefore the mixing of the states $|M|=2$ with the bright excitons is rather weak. A weak symmetry breaking is supported by the spin splitting of the predominantly bright excitons being equal to the splitting observed for the dot structures 1 and 2. The right panel of Fig. 5 shows the dot 3 Zeeman splittings between the predominantly bright (full symbols) and dark (open symbols) excitons as a function of B. Similarly to the case of dot 2, for the bright excitons in dot 3 ΔE depends quadratically on B for low fields and has a linear dependence at high B. The splitting ΔE between the ''dark'' excitons shows a linear B dependence in the field range in which these states can be resolved. All the results can be well described within the framework of the exciton fine structure developed

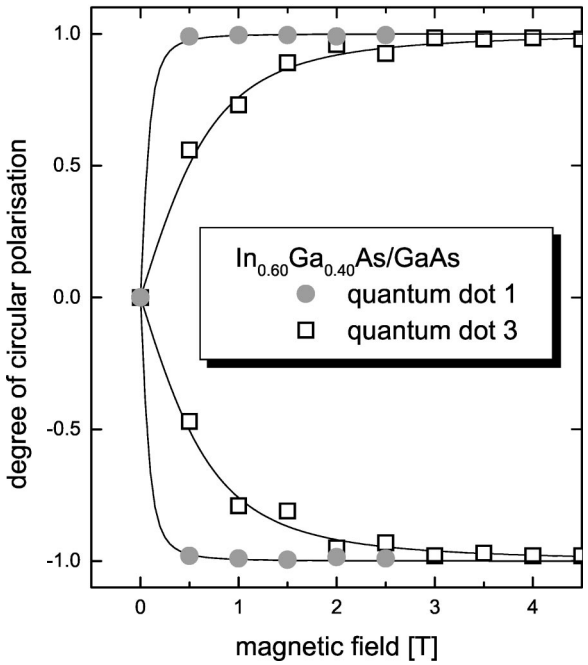

FIG. 6. Circular polarization P_C (as defined in the text) of the exciton emission of a highly symmetric and an asymmetric $In_{0.60}Ga_{0.40}As/GaAs$ single quantum dot (dots 1 and 3 of Fig. 3) as a function of the magnetic field. Symbols give the experimental data, and the lines the results of calculations using the fine structure parameters determined from the fit to the data in Fig. 4.

in Sec. II, as the comparison of the experimental data (symbols) with the results of the fits (lines) shows. However, no clear distinction concerning the relative importance of the short- and long-ranged exchange contribution to Δ_1 can be made from these data. We note, however, that a linear extrapolation of the ''dark'' exciton splitting to $B=0$ results in a splitting of about 50 μeV, which can arise only from the short-range interaction within the model discussed.

The different behaviors of the quantum dots also show up in the magnetic-field dependence of the circular polarization P_C of their emission. The degree of polarization P_C is defined by

$$P_C=\frac{I^+-I^-}{I^++I^-}, \tag{5}$$

where $I^{+/-}$ are the intensities of the $\sigma^{+/-}$ polarized components in the spectra. The symbols in Fig. 6 show the experimental data for the P_C as function of magnetic field for the two $In_{0.60}Ga_{0.40}As/GaAs$ quantum dots 1 and 3 of Fig. 3. For each dot two branches are shown corresponding to the two states within the bright exciton doublet: The one with $P_C>0$ shows the data of the low energy line (which becomes σ^+ polarized at high B), whereas the one with $P_C<0$ gives the data for the high-energy line (which becomes σ^- polarized at high B). Here we determined the $I^{+/-}$ by spectrally integrating over the emission lines. For dot 3 we have evaluated only the intensity data of the two emission features of strong intensity. Whereas dot 1 already shows a fully circularly polarized emission for very small magnetic fields, the

polarization transforms gradually from a linear to a circular one for dot 3. The behavior of dot 2 (not shown) is very similar to that of dot 3. For both these structures complete circular polarization is observed for $B>3$ T only. This transition reflects the restoration of the rotational symmetry by the magnetic field.

The P_C can be calculated from the exciton eigenstates in quantum dots with symmetry lower than D_{2d} (see Table III),

$$P_C(L_{1/2}) = \mp 1 \pm \frac{1}{r^2 + r\sqrt{1+r^2}+1}, \tag{6}$$

for the states $|L_{1/2}\rangle$ as defined in Table III. Here we have introduced the ratio r of the spin splitting of the $M=|1|$ excitons to the asymmetry energy: $r=(g_{e,z}+g_{h,z})\mu_B B/\Delta_1$. At low magnetic fields ($r\rightarrow 0$) the circular polarization vanishes, $P_C\rightarrow 0$, because the fine structure eigenstates are linear combinations of the circularly polarized excitons. At high fields the Zeeman interaction is much larger than the asymmetry exchange interaction ($r\rightarrow\infty$). Then the off-diagonal elements can be neglected, and the linearly polarized states $|L_{1/2}\rangle$ transform into circularly polarized states:

$$|L_1\rangle \rightarrow |+1\rangle,$$

$$|L_2\rangle \rightarrow |-1\rangle,$$

and consequently $P_C\rightarrow \pm 1$. The P_C calculated with the experimental quantum dot fine structure parameters are shown by the lines in Fig. 6, from which a good agreement with the experimental data is seen. For the present quantum dots the Zeeman splitting becomes comparable to the asymmetry energy δ_1 in dots 2 and 3 for small magnetic fields <1 T. For quantum dot 3, having the largest Δ_1, the P_C is already 50% at 0.5 T and 80% at 1 T, and approaches unity for $B>2$ T.

From studying a large number of single quantum dots of sample A, further insight into the behavior of the exchange energies can be obtained. A zero-magnetic field extrapolation of the dark exciton transition energies for dots exhibiting a quadruplet spin splitting gives the electron-hole exchange energy $\Delta_0=\delta_0+\gamma_0$, which is the energy difference between the bright and dark exciton doublets at $B=0$. We find strong variations of Δ_0 from about 100 to 250 μeV between the different dots. Furthermore, Δ_0 typically increases with the increasing energy of the emission within the $In_{0.60}Ga_{0.40}As/GaAs$ dot ensemble. This is an indication that the exchange energy increases with decreasing dot size. A major problem for understanding the electronic properties of self-assembled quantum dots is, however, the lack of knowledge of the dot size and shape, which limits the correlation of experimental data from optical studies with microscopic calculations.

A correlation between the exchange energy and dot size can be obtained in the following way: From scanning electron micrographs of an uncapped sample we determine a mean dot diameter of $D_M=22\pm 6$ nm. We assume that the energy of the luminescence of dots with a diameter D_M corresponds to the center E_M of the emission band of an unpatterned reference sample. Further, for simplicity, we assume

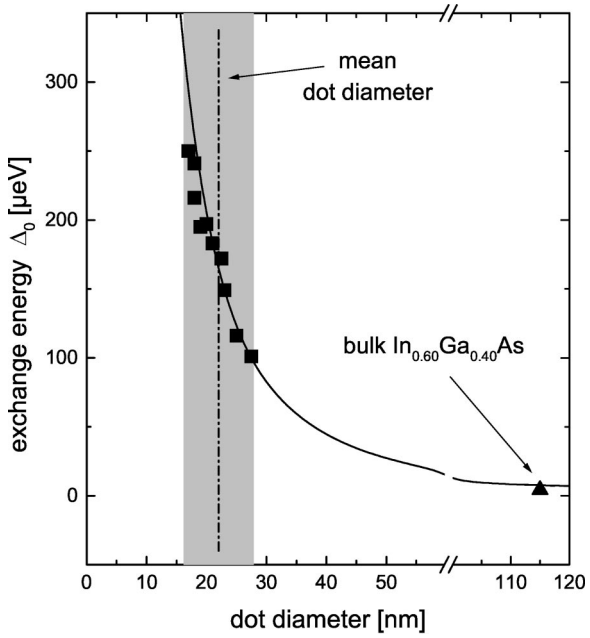

FIG. 7. Dot diameter dependence of the electron-hole exchange energy δ_0 for $In_{0.60}Ga_{0.40}As/GaAs$ self-assembled quantum dots. Symbols show the experimental data, and the line gives the results of variational calculations described in the text. The gray-shaded region indicates the variation of the quantum dot diameter around its mean value $D_M=22$ nm. D_M has been obtained from scanning electron microscopy.

that the dots have a cylindrical shape with a fixed height-to-width ratio of 1:3. Then we calculate the single-particle levels in such a cylinder by correlating the deviation of the emission energy from E_M with the deviation of its size from D_M for a particular single dot.

The dependence of Δ_0 on the dot diameter calculated in this way is shown in Fig. 7 by the squares. For comparison, $\Delta_0=4.3$ μeV for bulk $In_{0.60}Ga_{0.40}As$ is also shown there, which was determined from the experimental value of Δ_0 for bulk GaAs by scaling it with $1/a_B^3$ where a_B is the bulk exciton Bohr radius.[54] We find that the observed exchange energy increases strongly with decreasing dot size. In comparison to bulk Δ_0, it is enhanced by more than an order of magnitude. This increase shows the strong influence of quantum confinement on Coulomb interaction energies.[69,70] We have also performed detailed numerical calculations of Δ_0 in these quantum dots. For cylindrical dots, Δ_0 is given by the short-ranged contribution to the total exchange energy, and it is obtained from the probability of the electron and hole being at the same position as[82]

$$\delta_0 = \delta_0^{bulk} \times (\pi a_B^3) \times \int d^3r |\Psi_X(\vec{r}_e=\vec{r}_h)|^2. \tag{7}$$

Here δ_0^{bulk} is the exchange energy in the bulk, and Ψ_X is the exciton wave function, which is calculated by a multiparameter variational treatment.[83] For the dot shape we use a cylinder with a height to width ratio of 1:3 to represent it, as mentioned above. We find that the results for δ_0 are relatively insensitive to the shape assumed for the dot, but are

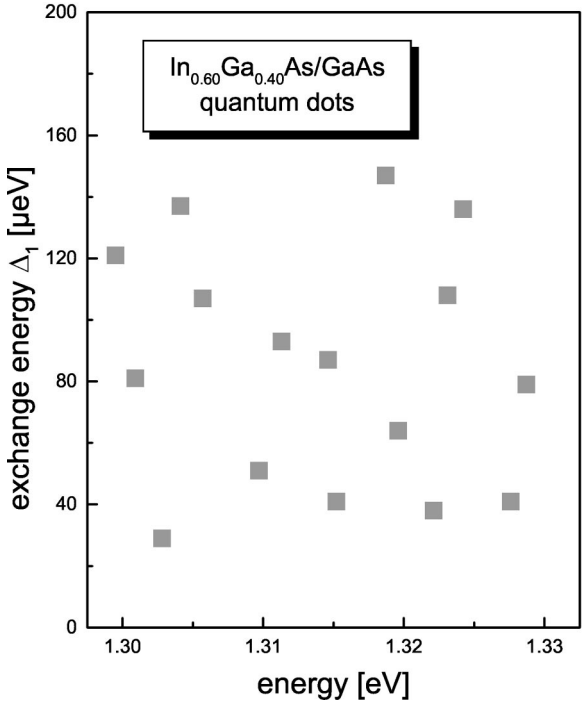

FIG. 8. Asymmetry induced exchange energy splitting $\Delta_1=\delta_1+\gamma_1$ of the bright excitons at $B=0$ as a function of the dot emission energy for $In_{0.60}Ga_{0.40}As/GaAs$ single quantum dots.

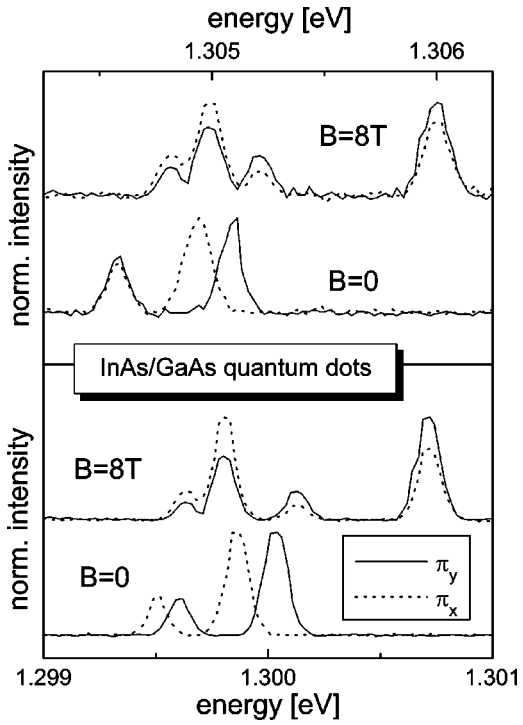

FIG. 9. The two panels show polarized photoluminescence spectra at zero magnetic field (bottom traces) and at $B=8$ T (top traces) of two different InAs/GaAs single quantum dots. For both field strengths the linear polarization degree of the emission was studied. These dots represent a fourth class of structures observed for sample B besides the three classes observed for sample A.

determined mainly by the dot volume. For these calculations we have used the following parameters: $m_e=0.0404$ and $m_h=0.35$ for $In_{0.60}Ga_{0.40}As$, and $m_e=0.0665$ and $m_h=0.35$ for GaAs. The band offsets are 468 meV for the conduction band and 230 meV for the valence band. For the dielectric constant we used a value of 15.0. The solid line in Fig. 7 shows the results of these calculations, which are in accord with the experimental data. To a good approximation, the exchange energy varies with the quantum dot diameter as $1/D^3$, which explains the observed strong variation of δ_0 with dot size.

In addition, the variation of the exchange energy Δ_1 (also given by the short- and long-ranged exchanges) can be determined from the spectroscopic data for quantum dots with broken D_{2d} symmetry. The data are plotted in Fig. 8 as functions of the dot emission energy at $B=0$. In contrast to Δ_0, Δ_1 characterizes the asymmetry of the structure and thus depends strongly on the dot shape. On the other hand, it has no direct correlation with the dot emission energy (i.e., the dot size).[84] From the spectroscopic data we find a maximum of 150 μeV for Δ_1, that varies within the experimental accuracy down to zero. Still the relative importance of the short- and long-ranged contributions to Δ_1 is not clear.

For the $In_{0.60}Ga_{0.40}As/GaAs$ quantum dots of sample A, no clear spectroscopic evidence was obtained that the observability of dark excitons arises from a complete geometric symmetry breaking. To obtain further insight, we have studied InAs quantum dots which were embedded in a GaAs matrix (sample B).[81] From scanning electron microscopy we find that the average diameter of these dots is about 15 nm, which is considerably smaller than for the $In_{0.60}Ga_{0.40}As/GaAs$ structures. Due to this smaller dot size, the excitonic properties should become more sensitive to shape asymmetries. In addition, the electron-hole exchange energy Δ_0 should be considerably enhanced. Summarizing the observations for all studied InAs/GaAs quantum dots, the same three classes of structures as for the $In_{0.60}Ga_{0.40}As/GaAs$ quantum dots are observed. In addition, we find another class exhibiting a different neutral exciton fine structure pattern.

Figure 9 shows photoluminescence spectra of two different InAs/GaAs single quantum dots belonging to this fourth class which were recorded at $B=0$ and 8 T. At both field strengths the emission has been analyzed with respect to its linear polarization. For the two dot structures, at zero field, there are two intense emission lines of orthogonal polarization on the high-energy side. Additional emission of weaker intensity appears on the low-energy side. For the first dot two spectral lines, which are fully linearly polarized as well, appear. For the second dot, however, a single line is observed only. Using the terminology developed in Sec. II, we conclude that the high-energy features originate from recombination of electron-hole pairs which consist predominantly of ± 1 excitons, while the character of the low-energy features is mostly ± 2 excitonlike. However, the observability of the ''dark'' states even at zero magnetic field shows that the symmetry of these dots must be strongly broken, and that an analysis of the fine structure using the Hamiltonian $\mathcal{H}_{exchange}$ is not sufficient. Still, for reasons of simplicity, we will continue the analysis within this framework. When ap-

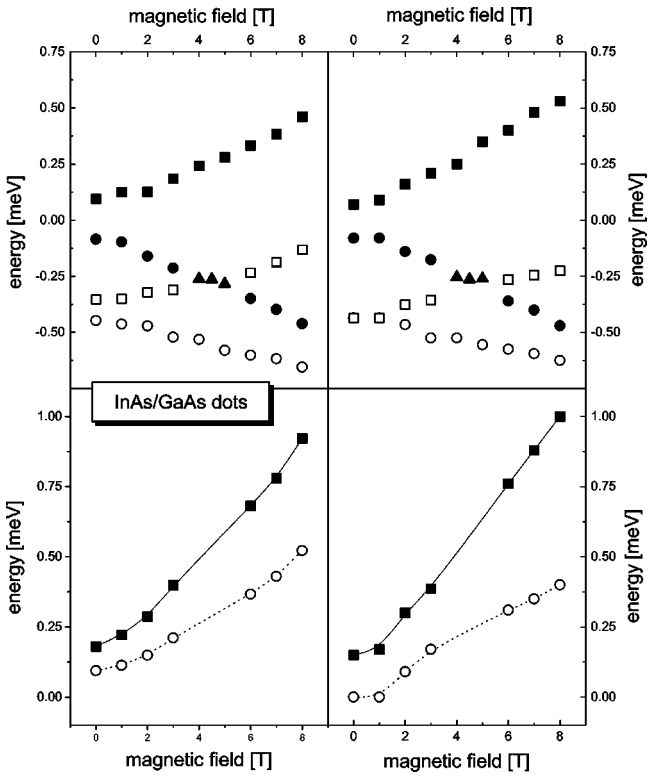

FIG. 10. Upper panels: exciton transition energies observed for the InAs/GaAs single quantum dots shown in Fig. 9 as functions of magnetic field. Lower panels: magnetic-field dependence of the exciton spin splitting observed for the InAs/GaAs single quantum dots. The lines serve as guides to the eye.

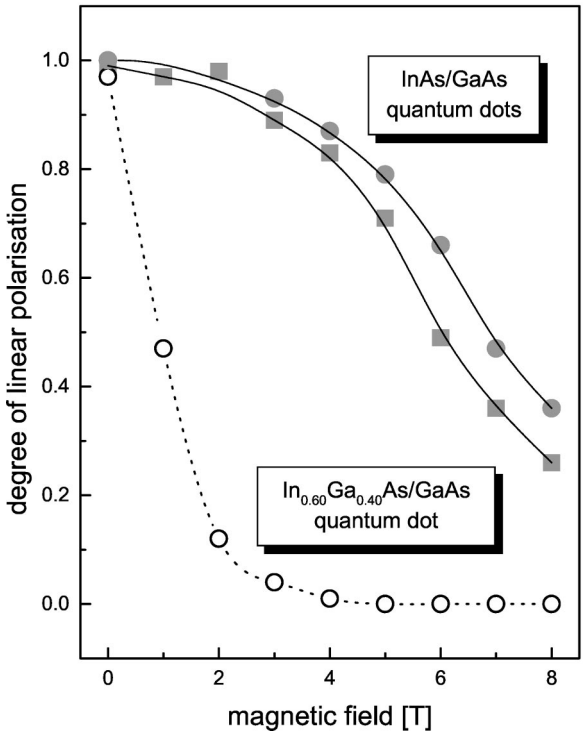

FIG. 11. Linear polarization P_L of the emission from the predominantly "bright" excitons in InAs/GaAs single quantum dots (sample B) with strongly broken symmetry as a function of the magnetic field in comparison to the polarization degree observed for an $In_{0.60}Ga_{0.40}As$/GaAs quantum dot (sample A) of reduced symmetry (dot 3 of Fig. 3). The lines are guides to the eye.

plying a magnetic field, the high- and low-energy lines are seen to split into doublets for both quantum dots. However, no transformation to a complete circular polarization is reached, in contrast to the $In_{0.60}Ga_{0.40}As$/GaAs quantum dots of sample A.

The upper panels in Fig. 10 show the observed transition energies as function of the magnetic field for the two InAs/GaAs quantum dots of Fig. 9. For clarity, again the energy of the center of the strong emission lines has been subtracted. From the splitting between the centers of the bright and dark exciton emission doublets at $B=0$ we obtain electron-hole exchange energies $\Delta_0 \approx 400$ and 450 μeV, respectively. We have made calculations of Δ_0 like those in Eq. (7) and find that $\Delta_0 = 325$ μeV for a dot radius of 15 nm. The emission energies of the two studied quantum dots are located above the center of the emission band of an unstructured reference sample, indicating dot radii smaller than the average one which will lead to a further enhancement of Δ_0. Thus the calculations are in reasonably good accord with the experimental data also for the InAs/GaAs quantum dots.

From the splitting of the upper doublet we obtain exchange energies of $\Delta_1 = 180$ and 150 μeV, respectively, for the two dot structures. More interestingly, for the splitting of the lower doublet, strong differences for δ_2, 90 μeV and 0, respectively, are found. As discussed above, within the model of Sec. II this splitting arises from the short-range exchange, which is believed to be small. This is confirmed by the results for the second dot, but the opposite is true for the first dot. In a nonzero magnetic field the splitting between the emission lines increases. For the first dot, the splittings for both doublets depend quadratically on B up to high fields, as seen from Fig. 10 (lower panels). The splitting between the high-energy features is ~ 0.8 meV at 8 T, while it is ~ 0.5 meV for the low-energy doublet. For the second dot, the behavior is qualitatively identical to the first dot for the predominantly bright excitons, whereas the splitting between the predominantly dark excitons shows a linear B dependence within the experimental accuracy.

Turning to the polarization of the emission from the sample B quantum dots, we found that even at the highest magnetic fields the emission exhibits a considerable linear polarization, as seen from the spectra at 8 T (Fig. 9). This means that the rotational symmetry cannot be restored by the fields available in the present experiments. Figure 11 shows the degree of linear polarization P_L defined by

$$P_L = \frac{I_{\parallel} - I_{\perp}}{I_{\parallel} + I_{\perp}}, \tag{8}$$

for the two InAs/GaAs quantum dots of Fig. 9 plotted versus the magnetic field. Here $I_{\parallel}$ and $I_{\perp}$ denote the (spectrally integrated) intensities of the emission polarized parallel and perpendicular to the [110] crystal direction. With increasing B the linear polarization decreases from 1 at $B=0$ to about 0.2 at 8 T. Using the eigenstates in Table III for calculating

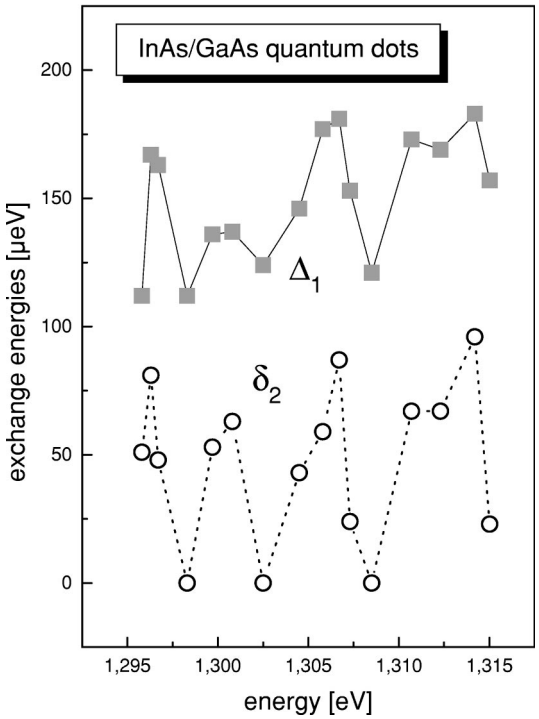

FIG. 12. Zero-magnetic-field exchange energy splittings Δ_1 between the predominantly bright (squares) and δ_2 between the predominantly dark (circles) exciton states in InAs/GaAs quantum dots exhibiting a strong symmetry breaking as functions of the center of the dot emission energy. The lines are guides to the eye.

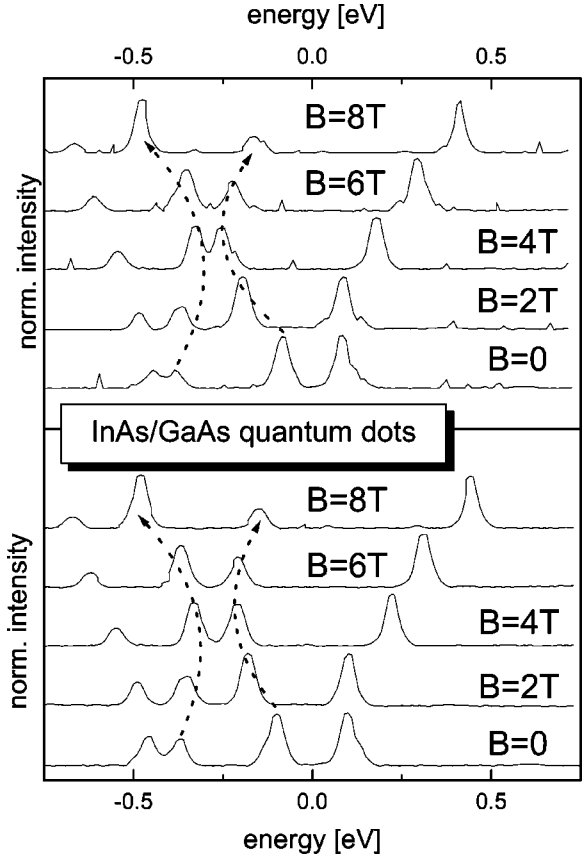

FIG. 13. Photoluminescence spectra of two different InAs/GaAs quantum dots with strongly broken symmetries for different magnetic fields. In the magnetic-field range between 2 and 6 T the $M=+2$ and $M=-1$ excitons approach and repel each other.

the linear polarization, we obtain a linear polarization clearly below 10%. Since Eq. (2) is based on the method of invariants, this estimate confirms that this analysis is not sufficient for discussing quantum dots with strongly broken symmetry.

Further insight is obtained by comparing the exchange energy splittings for several dots already exhibiting dark exciton emission at zero magnetic field. Figure 12 shows these energy splittings Δ_1 between the predominantly ''bright'' (squares) exciton features and δ_2 between the predominantly ''dark'' (circles) exciton features as function of the center of the dot emission energy at $B=0$. In contrast to the results in the $In_{0.60}Ga_{0.40}As/GaAs$ quantum dots, the Δ_1 now do not go down to zero but are always larger than 100 μeV, confirming a strong symmetry breaking. As expected, they also do not show any significant correlation with the dot emission energy.

The lack of correlation also holds for δ_2, which varies between 0 and 100 μeV. Within the method of invariants, the splitting can only arise from the short-range interaction, which would mean that the part of the Hamiltonian in Eq. (1) that is proportional to the third power of the hole momentum cannot be neglected. From the comparison of δ_2 with Δ_1 in Fig. 12, there seems to be a (weak) correlation of both quantities. When $\Delta_1=\delta_1+\gamma_1$ is large, there is a clear trend that δ_2 is large as well. Since $\delta_1<\delta_2$, we can conclude that the long-range interaction gives the dominant contribution to the splitting of the bright exciton doublet.

Figure 13 shows the photoluminescence spectra of two other quantum dots also belonging to this class of sample B dots. Since they are located in mesa structures with large lateral sizes ($\sim$300 nm as compared to $\sim$100 nm), their emission half-width is below 60 μeV, and therefore considerably smaller than that of the dots shown in Fig. 9. In both cases, around 4 T the emission line from the low-energy doublet that shifts to higher energies with increasing field and the line from the high energy doublet that shifts to lower energies approach each other. When they come in resonance, the two lines repel each other and exchange their characters: Below 3 T the low- (high-) lying line has a rather weak (strong) oscillator strength; above 5 T this ratio is reversed. A polarization analysis (not shown here) demonstrates that the behavior of the LP's is similar to that of the dots in Fig. 9.

The observed anticrossings occur due to the mixing of bright and dark excitons that arises from the strong symmetry breaking. The exciton angular momentum M is no longer a good quantum number in these structures; otherwise these states would not interact and cross each other. Figure 14 shows the observed transition energies of the InAs/GaAs quantum dots of Fig. 13 plotted versus the magnetic field. The minimum splitting between the two lines at the anticrossing point is about 100 μeV for the dot in the lower panel, and only 50 μeV for that in the upper panel. We note that for the dots in Fig. 9 the anticrossing should also occur in principle, but larger emission linewidths (in combination

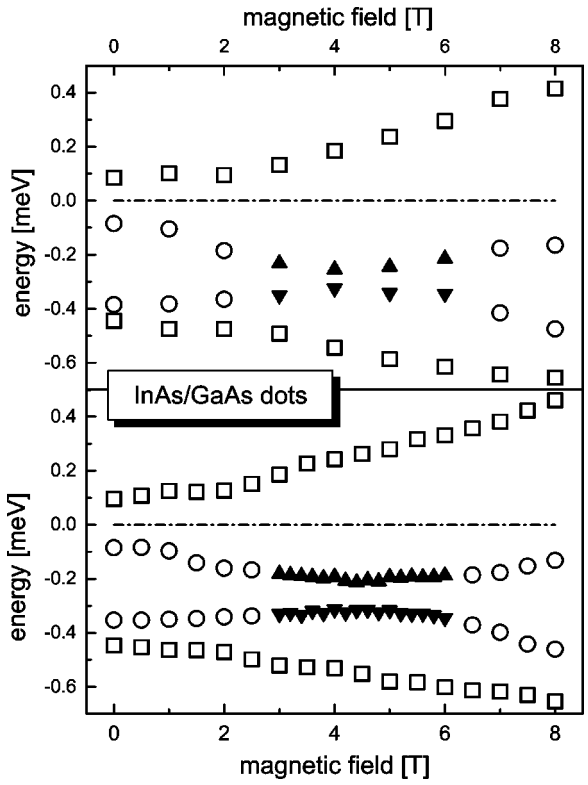

FIG. 14. Exciton transition energies of the two InAs/GaAs quantum dots shown in Fig. 13 vs the magnetic field.

with smaller splittings between the anticrossing branches) prevent its resolution in the spectra.

The minimum-energy splitting between the two anticrossing branches can be considered as an indicator of the strength of the symmetry breaking in the dots. Figure 15 shows this energy splitting versus the dot emission energy at $B=0$ for several sample B quantum dots. The splitting varies from 50 μeV (which is about the minimum value for which anticrossing can be resolved) to 125 μeV. Similar to the case of the asymmetry exchange energies Δ_1 and δ_2, there is no strong correlation here between the splitting and the emission energy.

2. Voigt configuration

a. Experimental data. The breaking of the quantum dot symmetry by a magnetic field can be tested by deliberately tilting the magnetic field out of the [001] direction.[26,69] For these studies we have selected $In_{0.60}Ga_{0.40}As/GaAs$ quantum dots from sample A that show a D_{2d} symmetry, i.e., in the Faraday configuration they show a behavior corresponding to that of dot 1 in Fig. 3. Figure 16 shows the photoluminescence spectra of such a symmetric $In_{0.60}Ga_{0.40}As/GaAs$ single quantum dot which were recorded in the Voigt configuration for varying magnetic-field strengths.[26] With increasing B the center of the emission features shifts to higher energies due to the diamagentic shift of the exciton. At $B=0$ a single emission line corresponding to emission from the $|M|=1$ excitons is observed. On its low-energy side an additional spectral line appears at $B=2$ T which originates

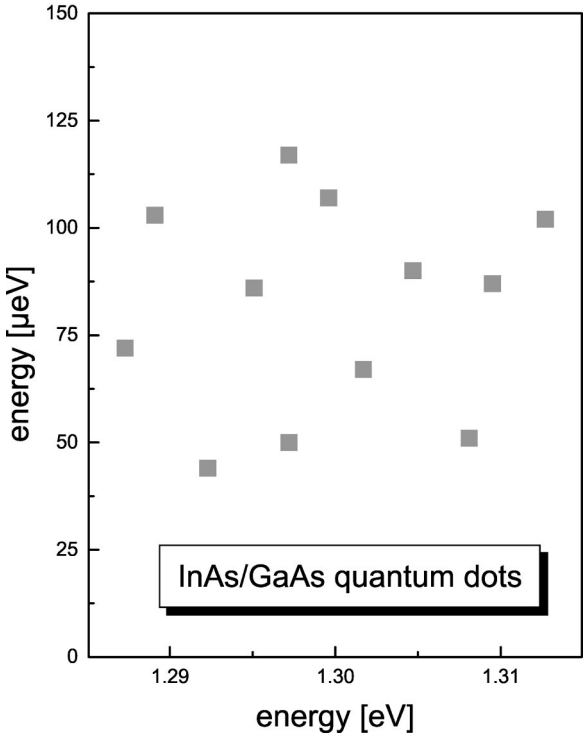

FIG. 15. Minimum-energy splitting between the two anticrossing branches originating from the hybridization of the excitons that have nominally $M=-1$ and $+2$ angular momenta in InAs/GaAs quantum dots plotted against the center of the dot emission energy at $B=0$.

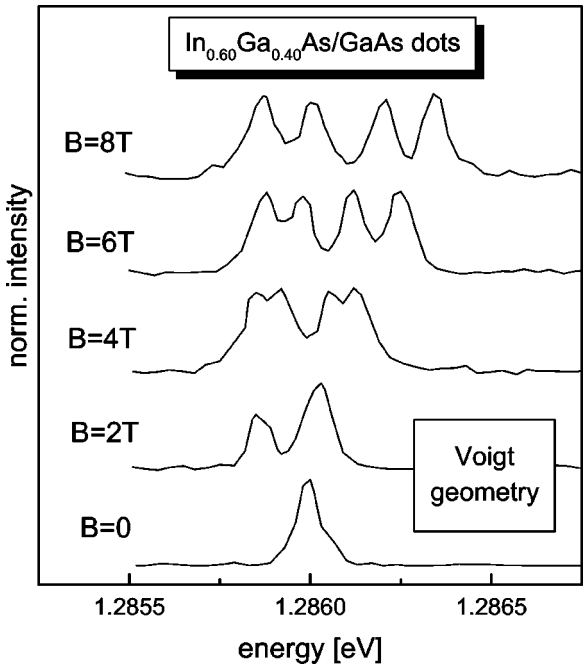

FIG. 16. Photoluminescence spectra of an $In_{0.60}Ga_{0.40}As/GaAs$ single quantum dot (sample A) recorded for varying magnetic-field strengths in the Voigt configuration. The dot belongs to a class of structures having D_{2d} symmetry.

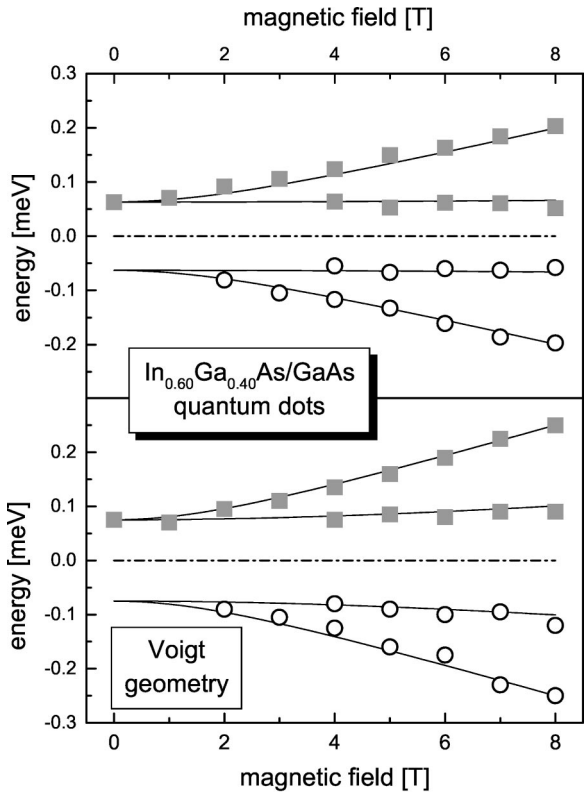

FIG. 17. Energies of the exciton transitions observed for two different $In_{0.60}Ga_{0.40}As/GaAs$ single quantum dots vs the magnetic field in the Voigt configuration (circles: dark excitons; squares: bright excitons at $B=0$). To focus on the fine structure, the diamagnetic shift of the center of emission has been subtracted in each case. The lines are fits to the data using the forms in Tables IV and V.

from the $|M|=2$ excitons at zero field. For higher fields each of the two emission lines splits into a doublet. The energy splitting between them increases with increasing B.

The strong emission intensity from the predominantly dark excitons, in particular at low fields, seems rather surprising because the off-diagonal matrix elements in the Hamiltonian which cause the mixing with the bright excitons are still small. Again this might be explained by the nonresonant, linearly polarized laser excitation by which excitons of all different spin orientations are generated. The relaxation between the spin states might be suppressed due to the discrete energy level structure in the dots.[75,76]

b. Discussion. Figure 17 shows the exciton transition energies versus the magnetic field in the Voigt configuration (pointing along the [100] direction) observed for two different, highly symmetric quantum dots. We have also rotated one of the dots (the one of Fig. 16) in steps of 45° around the heterostructure growth direction, so that B was also aligned along the [110] and [010] directions. Within the experimental accuracy we obtained the same results for these configurations, which gives a strong confirmation for the in-plane symmetry of the dot. In Fig. 17 we show only the data for the [100] orientation. To study only the fine-structure effects, the energy of the center of the emission features has been subtracted for each field strength.

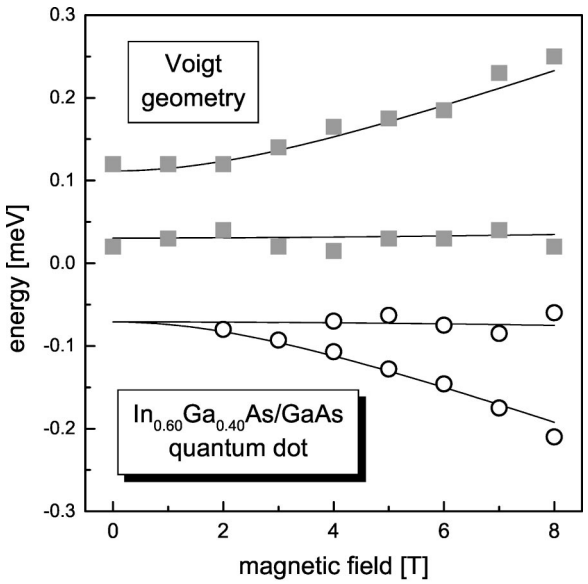

FIG. 18. Energies of the exciton transitions observed for an $In_{0.60}Ga_{0.40}As/GaAs$ single quantum dot vs the magnetic field in the Voigt configuration. This dot belogs to type 2 of sample A, which shows a linear polarization splitting at $B=0$, but no quadruplet splitting in magnetic field. The circles correspond to the dark excitons, and the squares to the bright excitons at $B=0$. To focus on the fine structure, the diamagnetic shift has been subtracted in each case. The lines are fits to the data using the forms in Tables IV and V.

The splitting of the energy levels follows the sketch in Fig. 2, as the comparison with the energies obtained by a fit to the data using the forms of Table IV (lines in Fig. 17) shows. The bright and dark excitons show no resolvable splittings at $B=0$ due to the high dot symmetry. Over the whole magnetic field range, the splitting between the two inner emission lines is mainly given by the exchange interaction Δ_0, and the Zeeman interaction has little influence on their energies. In contrast, it significantly changes the energies of the outer emission features. Here it should be noted that in quantum wells a quadruplet splitting cannot be observed in the Voigt configuration because experiments show that the in-plane hole g factor is about zero in these systems, which leads to a twofold degeneracy of the exciton states in the Voigt configuration (compare Tables IV and V).[63] Furthermore the electron g factors are found to be isotropic in quantum wells, in contrast to the present data. Thus the directionality dependence of the g factors in self-assembled quantum dots is considerably different from that in structures of higher dimensionality.

We have also studied $In_{0.60}Ga_{0.40}As/GaAs$ quantum dots of type 2, which show a linear polarization splitting at zero magnetic field (see Fig. 3) in the Voigt configuration. The observed transition energies are shown in Fig. 18, where we have again subtracted the diamagnetic shift. At zero field we observe two spectral lines separated by about $\Delta_1 = 100\ \mu$eV. These features are attributed to emission from the hybridized bright exciton states that are split mainly by long-range exchange interaction. The resolution of their splitting was possible because the studied dot was located in

a mesa structure with a large lateral size of 400 nm, resulting in a negligible influence of surface charges on the confinement potential. In a magnetic field the splitting between the two lines increases, with the higher-lying line shifting considerably to higher energies, whereas the energy of the low-energy line remains about constant.

Simultaneously the emission that arises from the dark exciton states at zero field appears in the spectra at about 2 T. First a single line is observed which then is seen to split into two features, where one line has a strong dispersion and the other one a small dispersion. Thus the behavior is quite similar to that of a highly symmetric dot except for the zero-field splitting of the bright excitons. It can be well described by the fine-structure Hamiltonian of Sec. II as the fits to the data using the forms of Tables IV and V demonstrate (the lines in Fig. 18). In particular, from extrapolating the energies of the low-lying emission lines to zero magnetic field, no significant splitting δ_2 of the dark exciton doublet is found for this quantum dot. This indicates that here the asymmetry splitting due to the short-range exchange interaction can be neglected.

B. Fine structure of charged excitons

1. Faraday configuration

a. Spectroscopic data. Now we want to focus on the third sample type, which were InAs quantum dots embedded in an $Al_{0.30}Ga_{0.70}As$ matrix (sample C). The average diameter of these dots is about 20 nm. From studying a large number of quantum dots, all sample C structures can be categorized in the following way: We find sets of quantum dots, the behavior of which can be described in the framework given in Sec. IV A for neutral excitons. However, we also observe a further class of dots, on whose fine structure we will concentrate in the following.[81] For these dots, strong phonon replicas appear in the emission spectra (not shown): The spectral features observed at energies around the *s* shell are identically repeated at higher energies. Their high energy shift is typically 36–37 meV, which is the energy of the GaAs LO phonon. The emission intensity of these replicas is almost that of the *s*-shell emission. Note that the features cannot be explained as transitions from the first excited dot shell: (a) The first excited shell would show a strong splitting in the magnetic field due to the lifting of its orbital angular momentum degeneracy by *B*. One component would shift strongly to higher energies, while the other would show a low-energy shift at small *B*.[85] No such behavior is observed for the high-energy lines. Instead, their magnetic-field shift is parallel to that of the *s*-shell features. (b) Furthermore, the spin splitting is exactly identical to that observed for the spectral lines at the *s*-shell energies, while for *p*-shell excitons a spin splitting different from that of a ground-state exciton would be expected.

For these $InAs/Al_{0.30}Ga_{0.70}As$ quantum dots with a strong coupling to LO phonons, additional classes of structures have to be introduced to capture all the structures of sample C. The two panels in Fig. 19 show the photoluminescence spectra of two different sample C InAs single quantum dots surrounded by $Al_{0.30}Ga_{0.70}As$, which show a quadruplet splitting in a magnetic field. The spectra were recorded for varying magnetic fields from $B=0$ up to 8 T. The emission of dot 1 (top panel) reminds one of the behavior observed for the $In_{0.60}Ga_{0.40}As/GaAs$ quantum dot 3 in Fig. 3: At $B=0$ a single emission line is observed which then splits into a quadruplet. However, in contrast to the sample A quantum dot, no indications of a linear polarization splitting at $B=0$ are found. Within the experimental accuracy the emission is circularly polarized. Most remarkably, after subtracting the diamagnetic shift the Zeeman splitting of the bright and the dark excitons is symmetric around the $B=0$ emission energy. This can be seen in Fig. 20, where the transition energies of two different $InAs/Al_{0.30}Ga_{0.70}As$ dots with such a splitting pattern are plotted against the magnetic field.

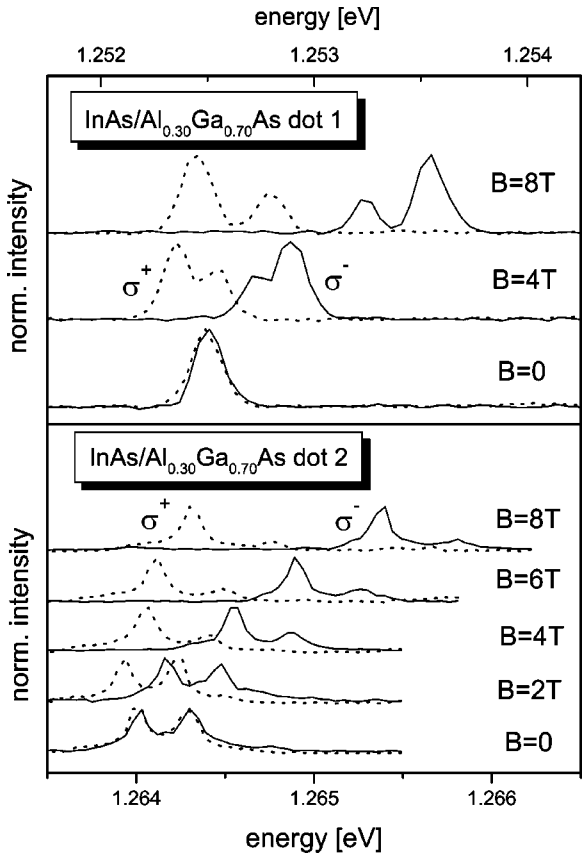

FIG. 19. The two panels show the circularly polarized photoluminescence spectra of two different InAs single quantum dots embedded in an $Al_{0.30}Ga_{0.70}As$ matrix for different magnetic fields (Faraday configuration).

In addition, another class of quantum dots is observed which shows a doublet splitting at $B=0$ (lower panel in Fig. 19). The splitting between the two spectral features is about 0.3 meV. In contrast to the InAs/GaAs quantum dots discussed in Sec. IV A, the intensities of the two split emission lines are about equal at $B=0$. Each of the two lines splits into a doublet in a magnetic field. The energy splitting is the same for the two doublets, but the intensity of the higher-lying doublet decreases drastically in comparison to that of the low-lying one. The σ^--polarized contribution originating from the low-energy feature as well as the σ^+-polarized line

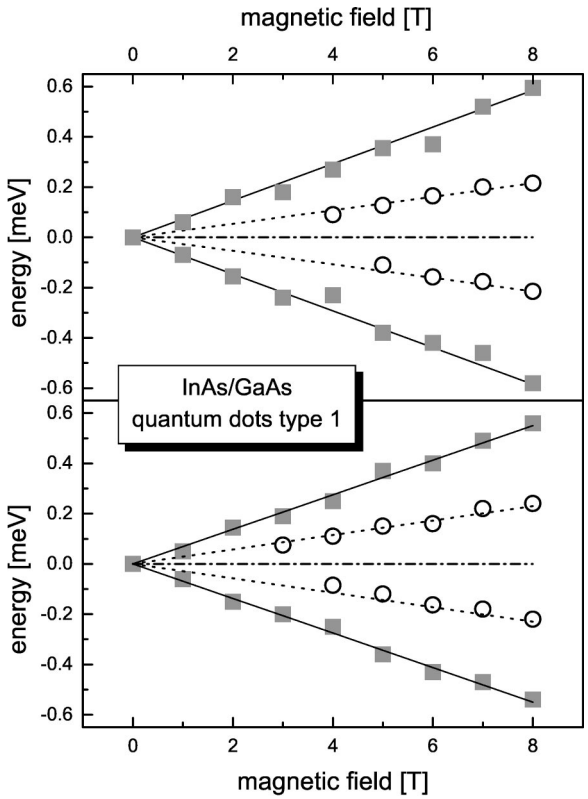

FIG. 20. The figure gives the exciton transition energies plotted against magnetic field for two different $InAs/Al_{0.30}Ga_{0.70}As$ quantum dots that show a single emission line at $B=0$ (see the upper panel of Fig. 18). Symbols give the experimental data, and lines the results of fits to the data.

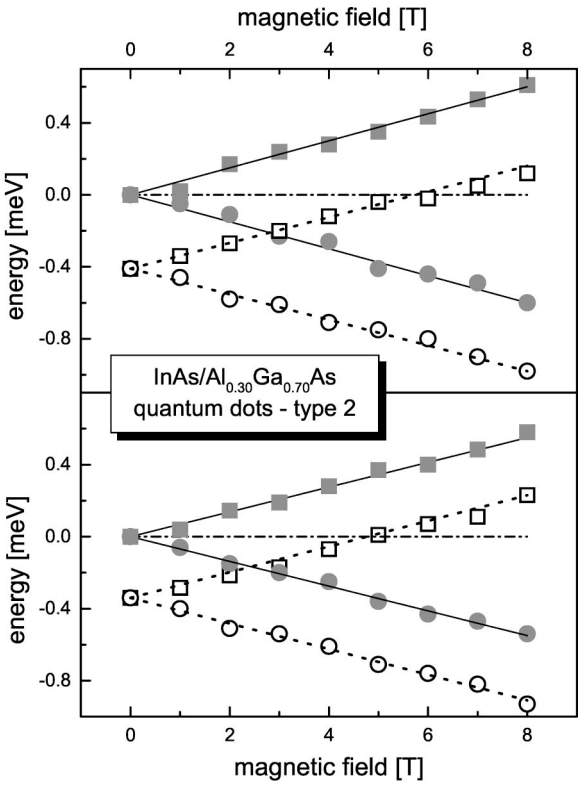

FIG. 21. Exciton transition energies plotted against magnetic field for two different $InAs/Al_{0.30}Ga_{0.70}As$ quantum dot with a zero-field doublet splitting (see the lower panel in Fig. 17). Symbols give the experimental data, and lines the results of fits to the data.

from the high-energy feature seem to cross each other without any noticeable interaction. The emission from this dot shows a circular polarization for all magnetic field strengths.

From these spectroscopic data one might conclude that two independent quantum dots are studied in this case. However, the same behavior, in particular, roughly the same splitting between the two zero-field lines, was observed for about 20% of the single quantum dots studied from sample C. Due to the dot inhomogeneities it is very unlikely that such a systematic behavior can arise from two quantum dots within a mesa structure. The observed behavior also cannot be explained by the appearance of neutral and charged excitons in the spectra, because the binding energy of a charged exciton complex is considerably larger than the observed energy splitting at $B=0$, as spectroscopic studies as well as detailed calculations on similar quantum dot systems show.[36,38,40,46,86] Further, from the equal spin splittings of the two emission lines and from the magnetic-field dependence of their intensities, the low-energy feature cannot be attributed to emission from predominantly dark excitons.

b. Discussion. First we will concentrate on quantum dots with a quadruplet splitting in a magnetic field emerging from a single line at $B=0$. The observation of a quadruplet splitting for these dots clearly indicates that the symmetry is broken in them. If the quantum dots would be occupied by a neutral exciton, there should be an exchange energy splitting Δ_0 between the bright and dark exciton doublets. The absence of such a splitting can only be explained by assuming that a free excess carrier is contained in the dots, so that after laser excitation charged excitons, either X^- or X^+ forms. In this case all exchange interaction energies $\delta_i, i=0,1,2$ and $\gamma_i, i=0,1$ are zero.[87] Further, for charge neutral exciton complexes the emission should show a linear polarization splitting, at least at low magnetic fields, which is in contrast to the experimental observations. The assumption of a charge in the system is also supported by the prominent appearance of phonon replica in the spectra, because in this case the coupling to phonons is much stronger than for a charge neutral system.

Generally the excess carriers in the quantum dots can have different origins. The first reason might be the nonresonant laser excitation. Due to their different mobilities, electrons and holes will have different carrier capture rates into the dot, leading to an imbalance of charge. Second, there might be an impurity in the dot surrounding. Typically, nominally undoped GaAs-based structures exhibit a residual *p*-type background doping. However, a definite assessment cannot be made for a single quantum dot because its behavior might be determined by a single impurity in its environment which can be a donor or an acceptor resulting in the formation of either X^- or X^+.

The different charged exciton configurations which are formed in the dot depend on the relaxation rates of the optically injected carriers into their ground states: As discussed above, earlier studies on single quantum dots indicate that

spin relaxation might be strongly suppressed, which was attributed to the discrete energy-level structure. Very recently this observation was confirmed by time-resolved studies of excitons in the quantum dot ground shell.[75,76] Depending on the carrier type, spins can relax through different mechanisms, which vary with the dimensionality of the studied system: The spin of an exciton can flip via the long-range exchange interaction only. For the spin-flip of an electron three different mechanisms exist:[55] In the Bir-Aronov-Pikus mechanism a spin-flip occurs via electron scattering at holes or at paramagnetic impurities. In the Dyakonov-Perel mechanism spin relaxation occurs due to a spin splitting of the conduction band for wave numbers $k \neq 0$ in crystals with broken center symmetries. Finally, in the Elliot-Yafet mechanism a mixing of the wave functions occurs for $k \neq 0$ because of band mixing arising from the $k \cdot p$ interaction. For a hole spin, the relaxation typically is considerably faster than for an electron due to the strong spin-orbit interaction. However, the actual relaxation rate depends on the strength of the localization potential. A comprehensive picture of the spin relaxation in quantum dots is still missing. Considering the different relaxation mechanisms, it is very likely that it will vary strongly with the quantum dot under study due to the strong variations of their symmetry properties.

Let us first consider a charged exciton confined in an $InAs/Al_{0.30}Ga_{0.70}As$ dot in which fast spin-flip processes can take place, as might be the case for X^+. Then the carriers relax rapidly toward their ground-state levels. If an equilibrium carrier is contained in the dot, a charged exciton in its ground state is formed. As was discussed in Sec. II, all fine-structure energies vanish, and the $B=0$ emission shows no splitting. In a magnetic field the emission splits into a doublet. However, if the dot symmetry is broken, for these dots a mixing of exciton states with $|M|=1$ and 2 occurs. As a consequence, four transitions with a symmetric energy splitting become observable in magnetic field (dot 1 in Fig. 19). The splitting between the emission lines of strong and weak intensities shows a linear dependence on the magnetic field. Here we again want to emphasize that only the observation of a fine-structure splitting (respectively its absence) is a clear proof of the neutrality of the exciton (the formation of a charged exciton complex).

Let us turn now to the discussion of the $InAs/Al_{0.30}Ga_{0.70}As$ quantum dots with a doublet splitting at $B=0$ by considering a charged dot, in which the excess charge can block spin relaxation. Due to the expected long spin relaxation times, this situation might be obtained if the dot contains an excess electron, so that an X^- complex is formed. If the dot is populated by two electrons having opposite spins and a hole, all carriers can relax into their ground states. If, on the other hand, the two electrons have parallel spins, the one electron in the *s* shell prevents the relaxation of the second one from the *p* shell. The Coulomb interaction energies for this configuration will be different from those in the first configuration. This energy difference will be reflected at $B=0$ in the emission of the *s*-shell exciton.

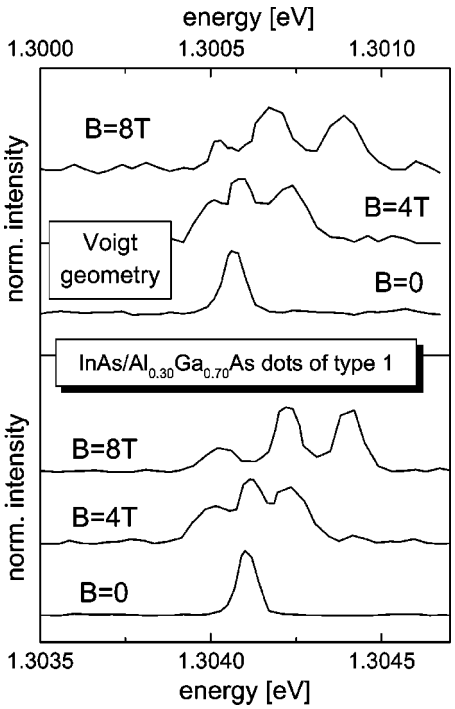

FIG. 22. Photoluminescence spectra of two different $InAs/Al_{0.30}Ga_{0.70}As$ quantum dots of high symmetry for different magnetic fields aligned in the Voigt geometry.

Figure 21 shows the magnetic-field dependence of the transition energies of two different sample C quantum dot with a zero-field doublet splitting, as in the lower panel of Fig. 19. We find ~ 300 and 400 μeV, respectively, for this energy splitting. Since the two emission features originate from recombination of an *s*-shell exciton, their spin splittings are equal. In general, the fine structure in the spectrum might be complicated further because the exciton in the ground shell might exhibit a fine-structure splitting similar to that of a neutral exciton. As mentioned above, no indications for a anticrossing of the high-energy feature originating from the lower line at $B=0$ and the low-energy feature from the higher line is observed with increasing magnetic field. The presented explanation for the recorded spectra gives a natural explanation for this crossing.

Finally we need to discuss the strong changes of the emission intensities from this sample C dot in a magnetic field, which indicates a strong-field dependence of the spin relaxation: The spin relaxation bottleneck obviously is softened by a magnetic field. This might be related to the transformation of the discrete quantum dot energy-level spectrum to a quasicontinuous one, because a magnetic field lifts the degeneracy of energy levels with positive and negative angular momenta in cylindrical dots. However, while the observed behaviors for type-1 InAs quantum dots in an $Al_{0.30}Ga_{0.70}As$ matrix can be uniquely attributed to charged excitons, there is still a lack of understanding concerning the formation of different excitonic spin configurations, as discussed here for type 2 dots. Therefore, in a next step quantum dot spectroscopy needs to address the problem of spin relaxation in the dot structures.

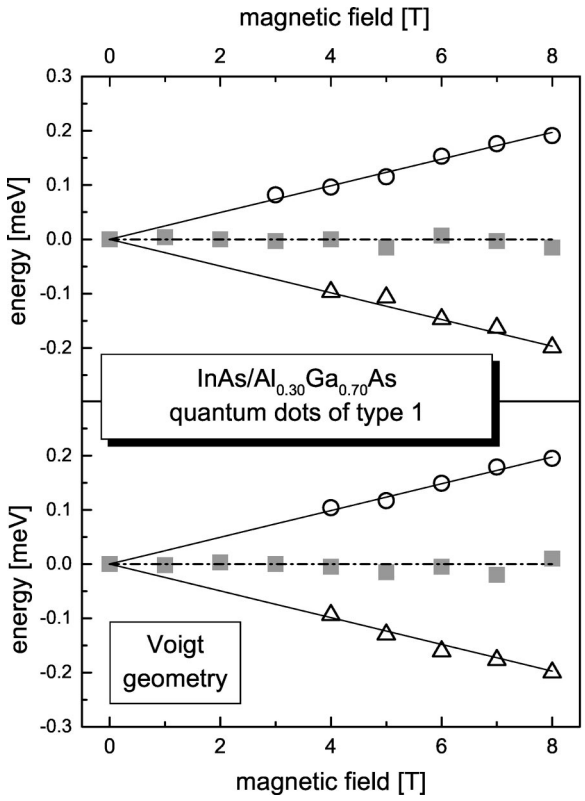

FIG. 23. Exciton transition energies of the two $InAs/Al_{0.30}Ga_{0.70}As$ quantum dots shown in Fig. 19 vs the magnetic field (Voigt geometry). Symbols give the experimental data, and lines give the results of fits to the data.

2. Voigt configuration

a. Spectroscopic data. Figure 22 shows photoluminescence spectra of symmetric $InAs/Al_{0.30}Ga_{0.70}As$ quantum dots of sample C (with an excitonic doublet splitting in the magnetic field) for varying B aligned normal to the heterostructure growth direction. The variation of the spectra with increasing B is strongly different from that observed in Fig. 16 for a charge neutral exciton. While there a line emerged on the low-energy side of the bright excitons, no such line shows up here. Instead, the single line observed at $B=0$ splits into a triplet in high magnetic fields. No indications of a quadruplet splitting are observed, as shown in Fig. 23, where the exciton transition energies are plotted as function of magnetic field, after subtracting the diamagnetic shift of the emission.

b. Discussion. The behavior observed in Fig. 23 gives another striking proof that the emission of these quantum dots originates from a charged exciton. The fine structure can be easily understood from that of a neutral exciton (Figs. 2 and 16) by setting the exchange energy Δ_0 to zero. At $B=0$, the energies of dark and bright excitons coincide. In a magnetic field, in general, a quadruplet splitting should be observed because the bright (dark) excitons shift to higher (lower) energies. However in Fig. 17 it was shown that the splitting between the two inner features is mostly given by Δ_0, which is zero here, and therefore the splitting between these two lines cannot be observed, their emissions overlap and combine to form the middle feature in the spectra in Fig. 22. The two outer spectral features correspond to the two outer emission lines in Fig. 16, the energies of which are considerably influenced by a magnetic field.

V. SUMMARY

In summary, we have studied the fine structure of exciton complexes in In(Ga)As/(Al)GaAs self-assembled quantum dots, which arises from the electron-hole exchange interaction and the interaction of the electron and hole spins with magnetic field, by single-dot photoluminescence spectroscopy. The experimental data have been analyzed by comparing them with a theoretical model. From the data a comprehensive picture of different scenarios for the exciton fine structure in quantum dots has been developed. We have shown that the symmetry of self-assembled quantum dots can vary strongly from a completely broken symmetry to a fully developed D_{2d} symmetry. Further we have found that in nominally undoped samples not only charge neutral dots are found but also dots which contain free charges, as might be expected from unavoidable background doping. As indicators of the quantum dot symmetry, the magnetic-field dependence of the exciton spin splitting as well as the polarization of the emission have been used.

ACKNOWLEDGMENTS

This work was financially supported by the Deutsche Forschungsgemeinschaft, the State of Bavaria, the National Research Council of Canada, the U.S. Office of Naval Research, and by the Defense Advanced Research Project Agency (DARPA). In part, it was carried out under the Canadian European Research Initiative on Nanostructures (CERION), which is supported by the European Commission (IST-FET program), the Canadian National Research Council and the Canadian Natural Sciences and Engineering Research Council. We gratefully acknowledge the expert technical assistance from M. Emmerling.

*Present address: Experimentelle Physik II, Universität Dortmund, Otto-Hahn-Straße 4, D-44227 Dortmund, Germany.

†Permanent address: Institute of Solid State Physics, Russian Academy of Sciences, 142432 Chernogolovka, Russia.

‡Present address: Department of Physics, Lebanon Valley College, Annville, Pennsylvania 17003.

[1] K. Brunner, U. Bockelmann, G. Abstreiter, M. Walther, G. Böhm, G. Tränkle, and G. Weimann, Phys. Rev. Lett. **69**, 3216 (1992); K. Brunner, G. Abstreiter, G. Böhm, G. Tränkle, and G. Weimann, *ibid.* **73**, 1138 (1994).

[2] J.-Y. Marzin, J.M. Gérard, A. Izraël, D. Barrier, and G. Bastard, Phys. Rev. Lett. **73**, 716 (1994).

[3] A. Zrenner, L.V. Butov, M. Hagn, G. Abstreiter, G. Böhm, and G. Weimann, Phys. Rev. Lett. **72**, 3382 (1994).

[4] M. Grundmann, J. Christen, N.N. Ledentsov, J. Böhrer, D. Bimberg, S.S. Ruvimov, P. Werner, U. Richter, U. Gösele, J. Hey-

denreich, V.M. Ustinov, A.Yu. Egorov, A.E. Zhukov, P.S. Kop'ev, and Zh.I. Alferov, Phys. Rev. Lett. **74**, 4043 (1995).
[5] D. Gammon, E.S. Snow, B.V. Shanabrook, D.S. Katzer, and D. Park, Science **273**, 87 (1996).
[6] D. Gammon, E.S. Snow, B.V. Shanabrook, D.S. Katzer, and D. Park, Phys. Rev. Lett. **76**, 3005 (1996).
[7] D. Gammon, S.W. Brown, E.S. Snow, T.A. Kennedy, D.S. Katzer, and D. Park, Science **277**, 85 (1997); S.W. Brown, T.A. Kennedy, D. Gammon, and E.S. Snow, Phys. Rev. B **54**, R17 339 (1996); D. Gammon, Al.L. Efros, T.A. Kennedy, M. Rosen, D.S. Katzer, S.W. Brown, V.L. Korenev, and I.A. Merkulov, Phys. Rev. Lett. **86**, 5176 (2001).
[8] R. Steffen, A. Forchel, T.L. Reinecke, T. Koch, M. Albrecht, J. Oshinowo, and F. Faller, Phys. Rev. B **54**, 1510 (1996).
[9] M. Nirmal, B.O. Dabbousi, M.G. Bawendi, J.J. Macklin, J.K. Trautman, T.D. Harris, and L.E. Brus, Nature (London) **383**, 802 (1996); Al.L. Efros and M. Rosen, Phys. Rev. Lett. **78**, 1110 (1997).
[10] S.A. Empedocles and M.G. Bawendi, Science **278**, 2114 (1997).
[11] U. Bockelmann, W. Heller, and G. Abstreiter, Phys. Rev. B **55**, 4469 (1997); W. Heller and U. Bockelmann, *ibid.* **55**, R4871 (1997).
[12] M. Bayer, T. Gutbrod, A. Forchel, V.D. Kulakovskii, A. Gorbunov, M. Michel, R. Steffen, and K.H. Wang, Phys. Rev. B **58**, 4740 (1998).
[13] E. Dekel, D. Gershoni, E. Ehrenfreund, D. Spektor, J.M. Garcia, and P.M. Petroff, Phys. Rev. Lett. **80**, 4991 (1998).
[14] L. Landin, M.S. Miller, M.E. Pistol, C.E. Pryor, and L. Samuelson, Science **280**, 262 (1998).
[15] A. Kuther, M. Bayer, A. Forchel, A. Gorbunov, V.B. Timofeev, F. Schäfer, and J.P. Reithmaier, Phys. Rev. B **58**, 7508 (1998); M. Bayer, A. Kuther, F. Schäfer, J.P. Reithmaier, and A. Forchel, *ibid.* **60**, R8481 (1999).
[16] Y. Toda, S. Shinomori, K. Suzuki, and Y. Arakawa, Phys. Rev. B **58**, 10 147 (1998).
[17] N. Bonadeo, J. Erland, D. Gammon, D. Park, D.S. Katzer, and D.G. Steel, Science **282**, 1473 (1998); N. Bonadeo, G. Chen, D. Gammon, D.S. Katzer, D. Park, and D.G. Steel, Phys. Rev. Lett. **81**, 2759 (1998).
[18] H. Kamada, H. Ando, J. Temmyo, and T. Tamamura, Phys. Rev. B **58**, 16 243 (1998); H. Kamada, H. Gotoh, H. Ando, J. Temmyo, and T. Tamamura, *ibid.* **60**, 5791 (1999).
[19] M. Bayer, A. Kuther, A. Forchel, A. Gorbunov, V.B. Timofeev, F. Schäfer, and J.P. Reithmaier, S.N. Walck, and T.L. Reinecke, Phys. Rev. Lett. **82**, 1748 (1999).
[20] V.D. Kulakovskii, G. Bacher, R. Weigand, T. Kümmel, A. Forchel, E. Borovitskaya, K. Leonardi, and D. Hommel, Phys. Rev. Lett. **82**, 1780 (1999).
[21] M. Sugisaki, H.-W. Ren, S.V. Nair, K. Nishi, S. Sogou, T. Okuno, and Y. Masumoto, Phys. Rev. B **59**, R5300 (1999).
[22] J. Puls, M. Rabe, H.-J. Wünsche, and F. Henneberger, Phys. Rev. B **60**, R16 303 (1999).
[23] F. Gindele, K. Hild, W. Langbein, and U. Woggon, Phys. Rev. B **60**, R2157 (1999); F. Gindele, U. Woggon, W. Langbein, J. M. Hvam, K. Leonardi, D. Hommel, and H. Selke, *ibid.* **60**, 8773 (1999).
[24] Y. Toda, O. Moriwaki, M. Nishioka, and Y. Arakawa, Phys. Rev. Lett. **82**, 4114 (1999).
[25] M.-E. Pistol, P. Castrillo, D. Hessman, J.A. Prieto, and L. Samuelson, Phys. Rev. B **59**, 10 725 (1999); L. Landin, M.-E. Pistol, C. Pryor, M. Persson, L. Samuelson, and M. Miller, *ibid.* **60**, 16 640 (1999).
[26] M. Bayer, O. Stern, A. Kuther, and A. Forchel, Phys. Rev. B **61**, 7273 (2000).
[27] P. Hawrylak, G.A. Narvaez, M. Bayer, and A. Forchel, Phys. Rev. Lett. **85**, 389 (2000).
[28] L. Besombes, K. Kheng, and D. Martrou, Phys. Rev. Lett. **85**, 425 (2000).
[29] M. Bayer, O. Stern, P. Hawrylak, S. Fafard, and A. Forchel, Nature (London) **405**, 923 (2000).
[30] R.J. Warburton, C. Schäflein, D. Haft, F. Bickel, A. Lorke, K. Karrai, J.M. Garcia, W. Schoenfeld, and P.M. Petroff, Nature (London) **405**, 926 (2000).
[31] O. Benson, C. Santori, M. Pelton, and Y. Yamamoto, Phys. Rev. Lett. **84**, 2513 (2000).
[32] A. Hartmann, Y. Ducommun, E. Kapon, U. Hohenester, and E. Molinari, Phys. Rev. Lett. **84**, 5648 (2000).
[33] E. Dekel, D.V. Regelman, D. Gershoni, and E. Ehrenfreund, W.V. Schoenfeld, and P.M. Petroff, Phys. Rev. B **62**, 11 038 (2000).
[34] P. Michler, A. Imamoglu, M.D. Mason, P.J. Carson, G.F. Strouse, and S.K. Buratto, Nature (London) **406**, 968 (2000).
[35] P. Michler, A. Kiraz, C. Becher, W.V. Schoenfeld, P.M. Petroff, L.D. Zhang, E. Hu, and A. Imamoglu, Science **290**, 2282 (2000).
[36] F. Findeis, A. Zrenner, G. Böhm, and G. Abstreiter, Phys. Rev. B **61**, R10 579 (2000).
[37] C. Santori, M. Pelton, G. Solomon, Y. Dale, and Y. Yamamoto, Phys. Rev. Lett. **86**, 1502 (2001).
[38] J.J. Finley, A.D. Ashmore, A. Lematre, D.J. Mowbray, M.S. Skolnick, I.E. Itskevich, P.A. Maksym, M. Hopkinson, and T.F. Krauss, Phys. Rev. B **63**, 073307 (2001).
[39] K. Matsuda, K. Ikeda, T. Saiki, H. Tsuchiya, H. Saito, and K. Nishi, Phys. Rev. B **63**, 121304 (2001).
[40] F. Findeis, M. Baier, A. Zrenner, M. Bichler, G. Abstreiter, U. Hohenester, and E. Molinari, Phys. Rev. B **63**, 121309 (2001).
[41] C. Becher, A. Kiraz, P. Michler, A. Imamoglu, W.V. Schoenfeld, P.M. Petroff, L. Zhang, and E. Hu, Phys. Rev. B **63**, 121312 (2001).
[42] G.S. Solomon, M. Pelton, and Y. Yamamoto, Phys. Rev. Lett. **86**, 3903 (2001).
[43] M. Sugisaki, H.-W. Ren, K. Nishi, and Y. Masumoto, Phys. Rev. Lett. **86**, 4883 (2001).
[44] D. Gammon, Al.L. Efros, T.A. Kennedy, M. Rosen, D.S. Katzer, D. Park, S.W. Brown, V.L. Korenev, and I.A. Merkulov, Phys. Rev. Lett. **86**, 5176 (2001).
[45] T.H. Stievater, X. Li, D.G. Steel, D. Gammon, D.S. Katzer, D. Park, C. Piermarocchi, and L.J. Sham, Phys. Rev. Lett. **87**, 133603 (2001).
[46] D.V. Regelman, E. Dekel, D. Gershoni, E. Ehrenfreund, W.V. Schoenfeld, and P.M. Petroff, Phys. Rev. B **64**, 165301 (2001).
[47] M. Baier, F. Findeis, A. Zrenner, M. Bichler, and G. Abstreiter, Phys. Rev. B **64**, 195326 (2001).
[48] E. Moreau, I. Robert, L. Manin, V. Thierry-Mieg, J.M. Gérard, and I. Abram, Phys. Rev. Lett. **87**, 183601 (2001).
[49] H. Kamada, H. Gotoh, J. Temmyo, T. Takagahara, and H. Ando, Phys. Rev. Lett. **87**, 246401 (2001).
[50] D.V. Regelman, U. Mizrahi, D. Gershoni, E. Ehrenfreund, W.V. Schoenfeld, and P.M. Petroff, Phys. Rev. Lett. **87**, 257401 (2001).

[51] For an overview of the extensive work on QD's, see, for example, L. Jacak, P. Hawrylak, and A. Wojs, *Quantum Dots* (Springer-Verlag, Berlin, 1998); D. Bimberg, M. Grundmann, and N. Ledentsov, *Quantum Dot Heterostructures* (Wiley, New York, 1998); U. Woggon, *Optical Properties of Semiconductor Quantum Dots* (Springer-Verlag, Berlin, 1997); A.D. Yaffe, Adv. Math. **50**, 1 (2001).

[52] See, for example, L. Goldstein, F. Glas, J.Y. Marzin, M.N. Charasse, and G. LeRoux, Appl. Phys. Lett. **47**, 1099 (1985); P.R. Berger, K. Chang, P. Bhattacharya, J. Singh, and K.K. Bajaj, *ibid.* **53**, 684 (1988); D.J. Eaglesham and M. Cerullo, Phys. Rev. Lett. **64**, 1943 (1990), D. Leonard, K. Pond, and P.M. Petroff, Phys. Rev. B **50**, 11 687 (1994); R. Leon and S. Fafard, *ibid.* **58**, R1726 (1998).

[53] R. Kotlyar, T.L. Reinecke, M. Bayer, and A. Forchel, Phys. Rev. B **63**, 085310 (2001); M. Bayer, V.B. Timofeev, T. Gutbrod, A. Forchel, R. Steffen, and J. Oshinowo, *ibid.* **52**, R11 623 (1995).

[54] G.L. Bir and G.E. Pikus, *Symmetry and Strain Induced Effects in Semiconductors* (Wiley, New York, 1974).

[55] E. L. Ivchenko and G.E. Pikus, *Superlattices and other Heterostructures*, Springer Series in Solid-State Sciences, Vol. 110 (Springer-Verlag, Berlin, 1997).

[56] R.J. Elliott, Phys. Rev. B **124**, 340 (1961).

[57] R.S. Knox, Solid State Phys. **5**, 25 (1963).

[58] G.E. Pikus and G.L. Bir, Zh. Éksp. Teor. Fiz. **60**, 195 (1971) [Sov. Phys. JETP **33**, 108 (1971)]; **62**, 324 (1972) [**35**, 174 (1972)].

[59] M.M. Denisov and V.P. Makarov, Phys. Status Solidi B **56**, 9 (1973).

[60] K. Cho, Phys. Rev. B **14**, 4463 (1976).

[61] U. Rössler and H.R. Trebin, Phys. Rev. B **23**, 1961 (1981).

[62] M. Nakayama, Solid State Commun. **55**, 1053 (1985).

[63] H.W. van Kasteren, E.C. Cosman, W.A.J.A. van der Poel, and C.T. Foxon, Phys. Rev. B **41**, 5283 (1990).

[64] E. Blackwood, M.J. Snelling, R.T. Harley, S.R. Andrews, and C.T.B. Foxon, Phys. Rev. B **50**, 14 246 (1994).

[65] L.C. Andreani and F. Bassani, Phys. Rev. B **41**, 7536 (1990).

[66] T. Takagahara, Phys. Rev. B **47**, 4569 (1990); **62**, 16 840 (2000).

[67] Al. Efros, M. Rosen, M. Kuno, M. Nirmal, D.J. Norris, and M. Bawendi, Phys. Rev. B **54**, 4843 (1996).

[68] M. Franceschetti, L.W. Wang, H. Fu, and A. Zunger, Phys. Rev. B **58**, R13 367 (1998).

[69] M. Nirmal, D.J. Norris, M. Kuno, M.G. Bawendi, Al. Efros, and M. Rosen, Phys. Rev. Lett. **75**, 3728 (1995).

[70] M. Chamarro, C. Gourdon, P. Lavallard, O. Lublinskaya, and A.I. Ekimov, Phys. Rev. B **53**, 1336 (1996); U. Woggon, F. Gindele, O. Wind, and C. Klingshirn, *ibid.* **54**, 1506 (1996).

[71] We note that the following discussion will be modified considerably if heavy-hole–light-hole mixing is included. For example, the exciton basis is then formed by eight states, and the in-plane terms linear in the hole momentum can no longer be neglected.

[72] For the exciton spin splitting in semiconductor nanostructures, in particular in quantum wells, highly nonlinear dependences on the magnetic field are observed. That is, the Zeeman interaction of the carrier spins, in particular that of the hole, cannot be described by constant g factors. The physical origin of this behavior, is the strong modification of band mixing by a magnetic field which in turn determines the magnitude of the g factors. In general, electron and hole g factors are defined by linear extrapolations of the corresponding spin splittings to zero magnetic field. For self-assembled quantum dots of high symmetry, on the other hand, up to now linear dependences of the exciton spin splitting on B have been reported only, as the results presented here confirm. Thus over the whole magnetic field range constant values can be used for $g_{e,i}$ and $g_{h,i}$ in Eq. (4).

[73] See, for example, K. Kheng, R.T. Cox, Merle Y. d' Aubigné, F. Bassani, K. Saminadayar, and S. Tatarenko, Phys. Rev. Lett. **71**, 1752 (1993); G. Finkelstein, H. Strikhman, and I. Bar-Joseph, *ibid.* **74**, 976 (1995); H. Buhmann, L. Mansouri, J. Wang, P.H. Beton, N. Mori, L. Eaves, M. Henini, and M. Potemski, Phys. Rev. B **51**, 7969 (1995).

[74] P. Hawrylak, A. Wojs, and J.A. Brum, Phys. Rev. B **54**, 11 397 (1996); A. Wojs and P. Hawrylak, *ibid.* **55**, 13 066 (1997); G. Narvaez and P. Hawrylak, *ibid.* **61**, 13 753 (2000).

[75] M. Paillard, X. Marie, P. Renucci, T. Amand, A. Jbeli, and J.M. Gérard, Phys. Rev. Lett. **86**, 1634 (2001).

[76] J.M. Kikkawa, I.P. Smorchkova, N. Samarth, and D.D. Awschalom, Science **277**, 1284 (1997); J.A. Gupta, D.D. Awschalom, X. Peng, and A.P. Alivisatos, Phys. Rev. B **59**, R10 421 (1999).

[77] F. Schäfer, J.P. Reithmaier, and A. Forchel, Appl. Phys. Lett. **74**, 2915 (1999).

[78] J.P. McCaffrey, M.D. Robertson, P.J. Poole, B.J. Riel, and S. Fafard, J. Appl. Phys. **90**, 1784 (2001); S. Fafard, Z.R. Wasilewski, and M. Spanner, Appl. Phys. Lett. **75**, 1866 (1999); S. Fafard, Z.R. Wasilewski, C.N. Allen, D. Picard, M. Spanner, J.P. McCaffrey, and P.G. Piva, Phys. Rev. B **59**, 15 368 (1999); Z.R. Wasilewski, S. Fafard, and J.P. McCaffrey, J. Cryst. Growth **202**, 1131 (1999), and references therein.

[79] C.N. Allen, P. Finnie, S. Raymond, Z.R. Wasilewski, and S. Fafard, Appl. Phys. Lett. **79**, 2701 (2001) and references therein.

[80] For a discussion of the homogeneous linewidth of the exciton emission in quantum dots, see, for example, P. Borri, W. Langbein, S. Schneider, U. Woggon, R.L. Sellin, D. Ouyang, and D. Bimberg, Phys. Rev. Lett. **87**, 157401 (2001); D. Birkedal, K. Leosson, and J.M. Hvam, *ibid.* **87**, 227401 (2001); C. Kammerer, G. Cassabois, C. Voisin, C. Delalande, Ph.Roussignol, A. Lemaitre, and J.M. Gérard, Phys. Rev. B **65**, 033313 (2002); M. Bayer and A. Forchel, *ibid.* **65**, 041308 (2002).

[81] We note that for some $In_{0.60}Ga_{0.40}As/GaAs$ (respectively InAs/GaAs) quantum dots we also find indications of emission from charged exciton complexes, besides the neutral exciton emission. The results obtained for the magnetic field dependence of these spectral lines are identical to those obtained for the sample C dots described in Sec. IVB. The origin of the trion emission most probably lies either in unintentional background doping or in the nonresonant excitation in combination with different carrier capture rates for electrons and holes due to their different masses.

[82] R. Romestain and G. Fishman, Phys. Rev. B **49**, 1774 (1994).

[83] S.N. Walck and T.L. Reinecke, Phys. Rev. B **57**, 9088 (1998).

[84] There might be an indirect correlation of the asymmetry exchange energies and the dot size, because excitons in smaller quantum dots react to confinement potential asymmetries more sensitively than in larger structures. In Fig. 12 this might be reflected by the trend of increasing Δ_1 and δ_2 with increasing emission energy.

[85] M. Bayer, A. Schmidt, A. Forchel, F. Faller, T.L. Reinecke, P.A. Knipp, A.A. Dremin, and V.D. Kulakovskii, Phys. Rev. Lett. **74**, 3439 (1995); R. Rinaldi, P.V. Giugno, R. Cingolani, H. Lip-

sanen, M. Sopanen, J. Tulkki, and J. Ahopelto, *ibid.* **77**, 342 (1996).

[86] K. Hinzer, P. Hawrylak, M. Korkusinski, S. Fafard, M. Bayer, O. Stern, A. Gorbunov, and A. Forchel, Phys. Rev. B **63**, 075314 (2001).

[87] We note that we have also studied *n*-type modulation-doped $In_{0.60}Ga_{0.40}As/GaAs$ quantum dot samples, for which we find qualitatively the same fine-structure pattern of the charged exciton as we observe here in nominally undoped structures. Typically the linewidth of the single-dot emission is, however, larger in the doped systems than in the undoped ones, which we attribute to the influence of fluctuating charges at the donors on the dot confinement potential during the integration time of the spectra.